SIAM J. APPLIED DYNAMICAL SYSTEMS
Vol. 17, No. 3, pp. 2076–2105

Coexistence of Hamiltonian-Like and Dissipative Dynamics in Rings of Coupled Phase Oscillators with Skew-Symmetric Coupling*

Oleksandr Burylko†, Alexander Mielke‡, Matthias Wolfrum§, and Serhiy Yanchuk¶

Abstract. We consider rings of coupled phase oscillators with anisotropic coupling. When the coupling is skew-symmetric, i.e., when the anisotropy is balanced in a specific way, the system shows robustly a coexistence of Hamiltonian-like and dissipative dynamics in the phase space. We relate this phenomenon to the time-reversibility of the system. The geometry of low-dimensional systems up to five oscillators is described in detail. In particular, we show that the boundary between the dissipative and Hamiltonian-like regions consists of families of heteroclinic connections. For larger rings with skew-symmetric coupling, some sufficient conditions for the coexistence are provided, and in the limit of $N \to \infty$ oscillators, we formally derive an amplitude equation for solutions in the neighborhood of the synchronous solution. It has the form of a nonlinear Schrödinger equation and describes the Hamiltonian-like region existing around the synchronous state similarly to the case of finite rings.

Key words. phase oscillators, reversible systems, bifurcations, amplitude equations

AMS subject classifications. 34C14, 34C15, 34C28, 34C30, 37C80, 70H33

DOI. 10.1137/17M1155685

1. Introduction.

Many phenomena in nature can be studied using models of lattices of coupled oscillatory systems. Examples are interacting semiconductor lasers [64], neural networks [3, 55], mechanical systems [34], biological oscillators [67], and others. In the limit of weak coupling, the dynamics of each subsystem can be described by a scalar phase variable [32, 74], and the coupled system can be reduced to a lattice of phase oscillators. In this context, one-dimensional arrays with periodic boundary conditions have been studied extensively [18, 58, 44, 67, 25, 20, 71, 79, 78, 50, 76, 36]. The rotation symmetry of such a system is a source of rich dynamical behavior including rotating waves [55, 80, 28, 73, 79, 11, 49, 53, 77, 78, 29], heteroclinic cycles [2], symmetric chaos [19, 78, 50, 44, 80], chimera states [38, 1, 76, 7], or compactons [51]. As an application in neuroscience, bifurcation mechanisms

*Received by the editors November 13, 2017; accepted for publication (in revised form) by I. Belykh May 29, 2018; published electronically August 1, 2018.
http://www.siam.org/journals/siads/17-3/M115568.html
Funding: The first author received financial support from Erasmus Mundus (grant MID2012B895) for work in Humboldt University. The work of the second author was partially supported by DFG within Collaborative Research Center 910 through Project A5. The work of the third and fourth authors was partially supported by DFG within Collaborative Research Center 910 through Project A3.
†Institute of Mathematics, National Academy of Sciences of Ukraine, Tereshchenkivska Str. 3, 01601 Kyiv, Ukraine (burylko@yahoo.co.uk).
‡Weierstrass Institute, Mohrenstr. 39, 10117 Berlin, Germany, and Institute of Mathematics, Humboldt University of Berlin, Rudower Chaussee 25, 12489 Berlin, Germany (alexander.mielke@wias-berlin.de).
§Weierstrass Institute, Mohrenstr. 39, 10117 Berlin, Germany (matthias.wolfrum@wias-berlin.de).
¶Institute of Mathematics, Technical University of Berlin, Straße des 17. Juni 136, 10623 Berlin, Germany (yanchuk@math.tu-berlin.de).

in rings of coupled Hodgkin–Huxley type neurons with inhibitory and excitatory synapses were studied in [10, 62, 33, 75], where a complex dynamical scenario and multistability are reported. A specific coupling structure on a ring is the case of undirected nonlocal coupling to several nearest neighbors, where self-organized patterns of coherence and incoherence, so-called chimera states, have been discovered.

While for certain applications, such as molecular chains, the coupling of one element to its neighbors is symmetric with respect to reflection in space, for other systems the coupling is essentially directional. This happens, for instance, in laser systems with directional coupling through optical injection or in neuronal systems, where neurons are coupled in one direction via chemical synapses. As a result, there is a need for the theoretical understanding of the dynamical properties of rings with nonsymmetric (anisotropic) couplings.

In this work we focus on a specific case of the anisotropy, when the coupling matrix is skew-symmetric. This leads to a time-reversibility of the system. In general, a time-reversal symmetry $\mathcal{R}$ of a system $\dot{x} = G(x)$ is an involution $\mathcal{R}$ of the phase space satisfying

$$G(\mathcal{R}\Phi) = -\mathcal{R}(G(\Phi)) \tag{1}$$

and $\mathcal{R}^2 = id$, with id being the identical transformation. In particular, time-reversibility implies that $\mathcal{R}\Phi(-t)$ is a solution when $\Phi(t)$ is. It is well known that a time-reversal symmetry has far reaching consequences for the geometry of the phase space. Classical results on the existence of families of periodic solutions, elliptic fixed points, and invariant tori can be found in the review paper [40]. Remarkably, such dynamical features of conservative or Hamiltonian systems can in reversible systems coexist with dissipative dynamics. In the following, the terms "Hamiltonian-like" and "dissipative" are used to distinguish these dynamical features. Without giving a general definition of "Hamiltonian-like," its meaning is precisely described in each specific case in propositions.

Previously, Politi, Oppo, and Badii showed such dynamics in a three-dimensional laser system [52]. Globally coupled superconducting Josephson junction arrays were studied by Tsang et al. [70], who showed the coexistence of Hamiltonian-like and dissipative dynamics, with the Hamiltonian-like dynamics being nonhomotopic to zero. An infinite chain of locally coupled phase oscillators with reversible properties has been studied by Topaj and Pikovsky in [68] and an asymmetric ring by Pikovsky and Rosenau in [51]. The latter case corresponds to a particular case of our model (6), which will be introduced in subsection 3.2. Golubitsky, Krupa, and Lim proved the existence of families of periodic and quasi-periodic solutions in the Stokeslet model with time-reversal symmetry [26]. For general theoretical results on the dynamics of time-reversible systems, see [46, 21, 4, 59, 24, 42, 56, 23, 40, 9, 41, 81, 15, 12, 61, 65], the review [40] by Lamb and Roberts, and references therein.

The purpose of the present paper is to point out that the dynamics of chains of coupled phase oscillators with skew-symmetric coupling are characterized as well by the coexistence of Hamiltonian-like and dissipative behavior. For low-dimensional systems with specific coupling functions, we can provide a full description of the Hamiltonian-like regions as being foliated by periodic orbits (Propositions 5.1 and 5.2). For higher dimensions we can prove only a weaker form of Hamiltonian-like behavior. There, the families of periodic orbits do not cover open sets of the phase space, but we can show that a neighborhood of the synchronous state, which turns out to be an elliptic fixed point, is densely filled with invariant tori (Proposition 4.2). For

$N = 5$ we illustrate the complex structure of the phase space by a numerical study. Finally, we show that for a large number of oscillators in the vicinity of the elliptic fixed point the system can be approximated by a nonlinear Schrödinger equation as an amplitude equation, indicating again in another way a Hamiltonian-like behavior.

This paper is organized as follows. In section 2 the model for the ring of coupled phase oscillators as well as the system for phase differences are introduced. In section 3 we define synchronous solutions and rotating waves and provide conditions for their existence and asymptotic stability.

In section 4 we consider a system with skew-symmetric coupling and show that the phase space exhibits the coexistence of a Hamiltonian-like and a dissipative dynamics. In particular, the Hamiltonian-like dynamics emerge close to the synchronized state, and the dissipative regions are located around rotating waves with nonzero wave numbers. In section 5, global properties of low-dimensional (dimensions 3, 4, and 5) systems with a coupling function of Kuramoto–Sakaguchi type are studied in detail.

Section 6 considers specific cases when the reversible or conservative dynamics can occur in systems with nonidentical coupled oscillators. We show that the system with arbitrary frequency differences, skew-symmetric (resp., symmetric) coupling, and odd (resp., even) coupling function is divergence free, leading to the coexistence of periodic, quasi-periodic, and more complicated solutions. For some cases, the first integrals are computed. For a special constellation of natural frequencies (equally distributed) we show also the reversibility.

Finally, in section 7 we consider the dynamics in a neighborhood of the synchronous solution in the case of an infinite ring of identical oscillators ($N \to \infty$) when each oscillator is coupled with a finite number $2l$ of its neighbors. We conclude with a discussion in section 8.

2. Oscillator model with circulant coupling.

We consider the following translationally invariant ring of coupled phase oscillators with periodic boundary conditions:

$$\dot{\theta}_i = \omega_i + \sum_{j=1}^{N} K_j g(\theta_i - \theta_{i+j}), \quad i = 1, \dots, N, \tag{2}$$

where $\theta_i \in [0, 2\pi)$ are phase variables, ω_i are natural frequencies, $g(x)$ is a smooth 2π-periodic coupling function, K_j, $j = 1, \dots, N$, are coupling strengths, and all subscripts are assumed modulo N. The coefficient $K_N \equiv K_0$ determines the self-coupling. System (2) can be rewritten in a way similar to the Kuramoto system [37] as

$$\dot{\theta}_i = \omega_i + \sum_{j=1}^{N} K_{j-i} g(\theta_i - \theta_j), \quad i = 1, \dots, N,$$

and it describes a network of oscillators with coupling strengths given by the *circulant* coupling matrix

$$K = \operatorname{circ}(K_0, K_1, \dots, K_{N-1}) = \begin{pmatrix} K_0 & K_1 & \dots & K_{N-2} & K_{N-1} \\ K_{N-1} & K_0 & K_1 & \ddots & K_{N-2} \\ \vdots & K_{N-1} & K_0 & \ddots & \vdots \\ K_2 & \ddots & \ddots & \ddots & K_1 \\ K_1 & K_2 & \dots & K_{N-1} & K_0 \end{pmatrix}. \tag{3}$$

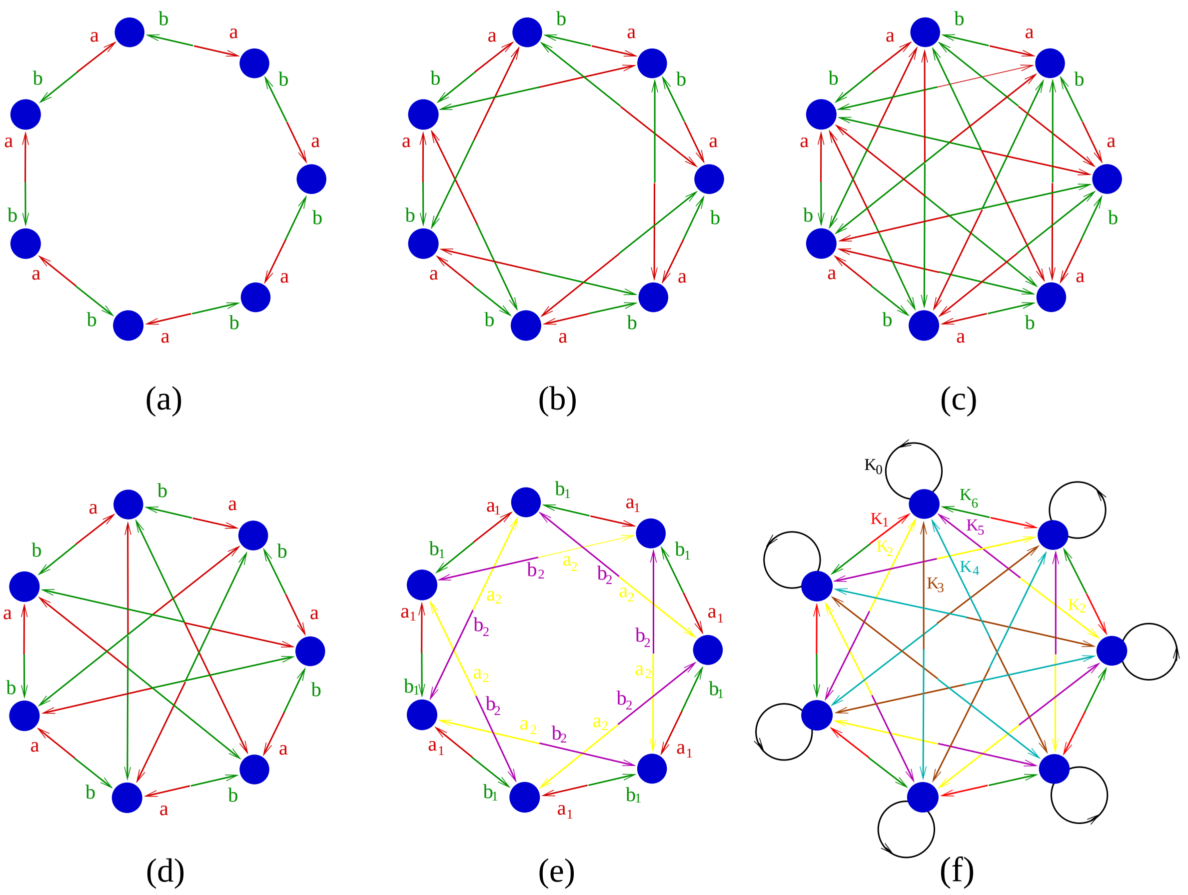

Figure 1. *Networks of seven asymmetrically coupled oscillators:* (a) *nearest-neighbor coupling* $l = 1$ *(see* (6)*),* (b) *second nearest-neighbor coupling* $l = 2$, (c) $l = 3$. *Networks in* (d)–(f) *are described by* (2)*, where* (d) $K_1 = K_3 = a$, $K_{-1} = K_{-3} = b$, *and* $K_2 = K_{-2} = 0$; (e) $K_1 = a_1 \neq K_2 = a_2$ *and* $K_{-1} = b_1 \neq K_{-2} = b_2$; (f) *arbitrary* K_j, $j = 0, \dots, 6$. *Different colors of arrows denote different coupling strengths.*

Figure 1 shows examples of networks with circulant connections for seven oscillators with coupling strengths $K_0, \dots, K_6$. Note that system (2) reduces to the classical Kuramoto model of globally coupled oscillators when $K_i = K_0$ for all $i = 1, \dots, N-1$ and $g(x) = \sin x$.

By introducing new variables

$$\varphi_i = \theta_1 - \theta_{i+1}, \quad i = 1, \dots, N-1, \tag{4}$$

we reduce (2) to the system in phase differences

$$\dot{\varphi}_i = \Delta_i + \sum_{j=1}^{N-1} K_j (g(\varphi_j) - g(\varphi_{i+j} - \varphi_i)), \quad i = 1, \dots, N-1, \tag{5}$$

where $\Delta_i = \omega_1 - \omega_{i+1}$, the subscripts are considered modulo N, and $\varphi_0 = 0$. We remark that the original system (2) possesses an $\mathbf{S^1}$ phase-shift symmetry

$$\theta_i \to \theta_i + \text{const}$$

that allows us to reduce it to the phase differences (5) where the reduced system has one fewer variables and does not have the $\mathbf{S^1}$ symmetry.

In the paper we mainly consider the case of identical oscillators $\Delta_i = 0$, except for section 6. Section 5 investigates examples of low-dimensional systems where $K_j = a$, $K_{-j} = b$, $j = 1, \dots, l$, $l < N/2$,

$$\dot{\theta}_i = \omega_i + a \sum_{j=1}^{l} g(\theta_i - \theta_{i+j}) + b \sum_{j=N-l}^{N-1} g(\theta_i - \theta_{i+j}), \quad i = 1, \dots, N. \tag{6}$$

The schematic diagram in Figure 1 illustrates examples of seven coupled oscillators with (a) $l = 1$, (b) $l = 2$, and (c) $l = 3$ where connections in different directions are marked by arrows of different color.

The system corresponding to (6) in phase differences has the form

$$\dot{\varphi}_i = \Delta_i + a \sum_{j=1}^{l} (g(\varphi_j) - g(\varphi_{i+j} - \varphi_i)) + b \sum_{j=N-1}^{N-l} (g(\varphi_j) - g(\varphi_{i+j} - \varphi_i)), \tag{7}$$

$i = 1, \dots, N-1$. In the case of identical oscillators $\omega_i = \omega$, $i = 1, \dots, N$, without loss of generality we can set $a = 1$ by rescaling the time. In this case and for specific coupling function $g(x) = -\sin(x - \alpha)$ we therefore deal with only two bifurcation parameters b and α.

3. Synchronous solution and rotating waves.

In the system of identical oscillators, the synchronous state exists where $\theta_i(t) = \theta_j(t)$ for all i, j, and t. In the system for phase differences (5) this solution corresponds to the fixed point $\varphi_i = 0$, $i = 1, \dots, N-1$. In fact, the reduced system (5) can have many different fixed points depending on the form of coupling function $g(x)$; however, some of them arise as a result of rotation symmetry of the network. Note that for identical oscillators the circulant structure of the coupling matrix induces an equivariance of the system with respect to the cyclic group Z_N acting by

$$\gamma : (\theta_1, \theta_2, \dots, \theta_N) \longmapsto (\theta_N, \theta_1, \dots, \theta_{N-1}).$$

For the reduced system (5) this symmetry is given as

$$\tilde{\gamma} : (\varphi_1, \varphi_2, \dots, \varphi_{N-1}) \longmapsto (-\varphi_{N-1}, \varphi_1 - \varphi_{N-1}, \dots, \varphi_{N-2} - \varphi_{N-1}).$$

One can check that solutions of (2) of the form

$$\left(\theta(t), \theta(t) - \frac{2\pi k}{N}, \dots, \theta(t) - \frac{(N-1)2\pi k}{N} \right), \tag{8}$$

$k = 0, \dots, N-1$, are equivariant under the symmetry action γ for arbitrary coupling function $g(x)$. Equation (8) represents *rotating wave* solutions with wave number k, where each oscillator is phase-shifted by $2\pi k/N$ with respect to the neighboring one. The corresponding solutions of the reduced system (5) are equilibria

$$\mathcal{M}_k = \left(\frac{2k\pi}{N}, \frac{4k\pi}{N}, \dots, \frac{2(N-1)k\pi}{N} \right). \tag{9}$$

The synchronous solution is therefore the rotating wave $\mathcal{M}_0$ with zero wave number. By substituting (9) into (5) one can see that the rotating waves with any wave number k exist for any choice of the coupling function g.

Proposition 3.1. *For any coupling function*[1] g, *system of coupled identical phase oscillators* (2) *possesses rotating wave solutions* (8) *with all possible wave numbers* k. *The corresponding solutions of the system in phase differences* (5) *are the equilibria* (9).

We note that system (5) can have other equilibria in addition to $\mathcal{M}_k$. Let us first point out the relationship between the system (2) and the corresponding system in phase differences (5). The following proposition shows that the Jacobian matrices of these two systems evaluated at the corresponding points share the same set of eigenvalues except the trivial one, which is induced by the phase-shift symmetry of the original system (2).

Proposition 3.2. *Let* A *and* B *be the Jacobian matrices of systems* (2) *and* (5), *respectively, that are evaluated at corresponding points* $(\theta_1, \dots, \theta_N)$ *and* $(\varphi_1, \dots, \varphi_{N-1})$, $\varphi_i = \theta_1 - \theta_{i+1}$ $(i = 1, \dots, N-1)$. *Then the following relation holds:*

$$\det(A - \lambda I_N) = -\lambda \det(B - \lambda I_{N-1}),$$

where I_N *is an* $N \times N$*-dimensional identity matrix.*

The additional zero eigenvalue of the matrix A corresponds to the neutral stability of each solution of the original system (6) along the eigenvector $v = (1, \dots, 1)$ and appears due to the phase-shift symmetry. The proof of Proposition 3.2 as well as Proposition 3.3 is in the appendix.

3.1. Stability of rotating waves. The following result establishes the spectrum of rotating waves $\mathcal{M}_k$.

Proposition 3.3. *Eigenvalues of the Jacobian matrix of system* (2) *evaluated at the rotating wave solution* $\mathcal{M}_k$ *are*

$$\lambda_m(\mathcal{M}_k) = \sum_{j=1}^{N-1} K_j \eta_{kj} \left(1 - e^{\imath \frac{2mj\pi}{N}}\right), \quad m = 1, \dots, N-1, \tag{10}$$

where $\imath = \sqrt{-1}$ *and* $\eta_{kj} = g'\left(\frac{2\pi k}{N} j\right)$.

Equality (10) implies that the system has $[N/2]$ complex conjugate pairs (the cases when $\operatorname{Im}\lambda = 0$ are also taken into account):

$$\lambda_{N-m}(\mathcal{M}_k) = \lambda_{-m}(\mathcal{M}_k) = \overline{\lambda}_m(\mathcal{M}_k), \tag{11}$$

where $\overline{\lambda}$ is the complex conjugate to λ. In particular, it holds $\operatorname{Im}(\lambda_{N/2}(\mathcal{M}_k)) = 0$ for any $\mathcal{M}_k$ when N is an even number.

The following result follows from Proposition 3.3 and summarizes the stability properties of $\mathcal{M}_k$.

[1] *Here and hereafter, we assume that* $g(\cdot)$ *is sufficiently smooth to guarantee the global existence of the solution, but we do not mention explicitly.*

Corollary 3.4. *The following statements hold true:*

- *If the inequality*
$$Re(\lambda_m(\mathcal{M}_k)) = \sum_{j=1}^{N-1} K_j \eta_{kj} \left(1 - \cos\left(\frac{2mj\pi}{N}\right)\right) < 0$$
holds for all $m = 1, \ldots, N-1$*, then the rotating wave* $\mathcal{M}_k$ *is asymptotically stable.*
- *If there exists an index* $1 \le m \le N-1$ *such that* $\mathrm{Re}(\lambda_m(\mathcal{M}_k)) > 0$*, then the rotating wave is unstable.*
- *If there exists an index* $1 \le m \le N-1$*,* $m \ne N/2$*, such that* $\mathrm{Re}(\lambda_m(\mathcal{M}_k)) = 0$*, then there exists a pair of complex conjugated eigenvalues*
$$\lambda_{\pm m}(\mathcal{M}_k) = \pm \imath \Omega_m, \quad \Omega_m = -\sum_{j=1}^{N-1} K_j \eta_{kj} \sin\left(\frac{2mj\pi}{N}\right).$$

Corollary 3.4 shows that the conditions $\mathrm{Re}(\lambda_m(\mathcal{M}_k)) = 0$ provide stability boundaries for the rotating waves and the synchronous solution $k = 0$. In the case when $\Omega \ne 0$, an Andronov–Hopf bifurcation can take place [30, 39, 63, 27].

Using the complex conjugacy $\nu_{-m} = \overline{\nu}_m$ we can rewrite real and imaginary parts of eigenvalues (10):

$$\begin{aligned} \mathrm{Re}\left(\lambda_m(\mathcal{M}_k)\right) = &\sum_{j=1}^{[(N-1)/2]} \left(K_j \eta_{kj} + K_{-j}\eta_{-kj}\right)\left(1 - \cos\left(\frac{2mj\pi}{N}\right)\right) \\ &+ \frac{1}{2}\left((-1)^N + 1\right)\left((-1)^{m+1} + 1\right) K_{N/2}, \end{aligned} \tag{12}$$

$$\mathrm{Im}\left(\lambda_m(\mathcal{M}_k)\right) = -\sum_{j=1}^{[(N-1)/2]} \left(K_j \eta_{kj} - K_{-j}\eta_{-kj}\right) \sin\left(\frac{2mj\pi}{N}\right), \tag{13}$$

where $[\cdot]$ denotes the integer part. Corollary 3.4 together with (12) shows that it is possible to observe a degenerate bifurcation with up to $[(N-1)/2]$ critical pairs of eigenvalues at the point $\mathcal{M}_k$.

Remark. System (5) has equilibria other than the origin and rotating waves (9). For example, it has fixed points $\widetilde{\Phi} = (\widetilde{\varphi}_1, \ldots, \widetilde{\varphi}_{N-1})$ with coordinates 0 and π ($\widetilde{\varphi}_i \in \{0, \pi\}$). It is easy to check that Jacobian matrix of the system (2) at the solution $\widetilde{\Theta}$ (corresponding to solutions $\widetilde{\Phi}$ of (5)) is not circulant. Therefore, the eigenvalues $\lambda_m(\widetilde{\Theta})$ cannot be described similarly to (10).

3.2. The model with different forward and backward connections. By applying the results of Corollary 3.4 to system (7) we obtain the following statements about particular cases, which are used in section 5.

Corollary 3.5. *The rotating wave solutions* $\mathcal{M}_k$*,* $k = 0, \ldots, N-1$*, of system* (7) *undergo a bifurcation if*

$$\mathrm{Re}(\lambda_m(\mathcal{M}_k)) = \sum_{j=1}^{l} (a\eta_{kj} + b\eta_{-kj}) \left(1 - \cos\left(\frac{2mj\pi}{N}\right)\right) = 0 \tag{14}$$

for some $1 \le m \le [(N-1)/2]$. *If, additionally, the inequality*

$$\Omega := \mathrm{Im}(\lambda_m(\mathcal{M}_k)) = -\sum_{j=1}^{l}(a\eta_{kj} - b\eta_{-kj})\sin\left(\frac{2mj\pi}{N}\right) \neq 0 \tag{15}$$

holds, then a pair of complex conjugate critical eigenvalues $\lambda_{\pm m} = \pm\imath\Omega$ *appears.*

Corollary 3.6. *The rotating wave solutions* $\mathcal{M}_k$ *of system* (7) *with nearest-neighbor coupling* ($l = 1$) *have all eigenvalues purely imaginary if the condition*

$$ag'(2k\pi/N) + bg'(-2k\pi/N) = 0 \tag{16}$$

is satisfied. If additionally $g'(2k\pi/N) \neq 0$, *then among these eigenvalues there are* $[(N-1)/2]$ *complex conjugated pairs.*

The solution $\mathcal{M}_k$ *is asymptotically stable when* $ag'(2k\pi/N) + bg'(2k\pi/N) < 0$.

The conditions (14) and (15) can be simplified at the synchronized solution $\mathcal{M}_0$ of (7) to the following form:

$$\mathrm{Re}(\lambda_m(\mathcal{M}_0)) = g'(0)(a+b)\sum_{j=1}^{l}\left(1-\cos\left(\frac{2mj\pi}{N}\right)\right) = 0, \quad m = 1,\dots,N-1, \tag{17}$$

$$\mathrm{Im}(\lambda_m(\mathcal{M}_0)) = -g'(0)(a-b)\sum_{j=1}^{l}\sin\left(\frac{2mj\pi}{N}\right) \neq 0. \tag{18}$$

The last multiplier on the right-hand side of (17) is always positive and the last multiplier on the right-hand side of (18) is nonzero because $m \neq 0$, $j \neq 0$. For the bifurcation of the synchronous solution we obtain the following conditions.

Corollary 3.7. *The synchronous solution* $\mathcal{M}_0$ *of system* (7) *with nearest-neighbor coupling* ($l = 1$) *has all eigenvalues purely imaginary if the condition*

$$a = -b \neq 0 \quad \text{or} \quad g'(0) = 0 \tag{19}$$

is satisfied. In the case $g'(0) = 0$, *all eigenvalues are zero.*

The solution $\mathcal{M}_0$ *is asymptotically stable when* $ag'(0) + bg'(0) < 0$.

An example when all eigenvalues are zero is the Kuramoto–Sakaguchi [57] coupling function $g(x) = -\sin(x-\alpha)$ for $\alpha = \pm\pi/2$, where a degenerate transcritical bifurcation occurs, since $g'(0) = -\cos(0-\alpha) = 0$.

In the case $a = b$ when the coupling is symmetric, the condition (14) reduces to

$$\sum_{j=1}^{l}(\eta_{kj} + \eta_{-kj})\left(1-\cos\left(\frac{2mj\pi}{N}\right)\right) = 0. \tag{20}$$

In particular, the condition holds for all k when the derivative of the coupling function is odd $g'(x) = -g'(-x)$. We have the following statements.

Corollary 3.8. *Let $a = b$ in (7) and the coupling function is even $g(x) = g(-x)$. Then the spectrum of all rotating wave solutions $\mathcal{M}_k$ is critical, i.e.,* $\mathrm{Re}(\lambda_m(\mathcal{M}_k)) = 0$ *for all $m = 1, \ldots, N-1$ and $k = 0, \ldots, N-1$.*

Corollary 3.9. *Let $a = -b$ in (7) and the coupling function is odd $g(x) = -g(-x)$. Then the spectrum of all rotating wave solutions $\mathcal{M}_k$ is critical.*

One can show that the system is divergence free for both Corollary 3.8 and Corollary 3.9.

4. Coexistence of Hamiltonian-like and dissipative dynamics in systems of coupled identical oscillators. In this section, we consider system (2) with arbitrary number N of coupled identical oscillators. We show that the phase space splits into regions with dissipative and Hamiltonian-like dynamics, provided the coupling is skew-symmetric, i.e., $K_j = -K_{-j}$.

For the skew-symmetric coupling, systems (2) and (5) can be written as follows:

$$\dot{\theta}_i = \omega + \sum_{j=1}^{[(N-1)/2]} K_j \left(g(\theta_i - \theta_{i+j}) - g(\theta_i - \theta_{i-j}) \right), \tag{21}$$

$$\dot{\varphi}_i = \sum_{j=1}^{[(N-1)/2]} K_j (g(\varphi_j) - g(\varphi_{-j}) - g(\varphi_{i+j} - \varphi_i) + g(\varphi_{i-j} - \varphi_i)) \tag{22}$$

with $i = 1, \ldots, N-1$. Note that $K_0 = 0$ as well as $K_{N/2} = 0$ when N is even.

Let us first show that system (22) is time-reversible.

Lemma 4.1. *System (22) has time-reversal symmetry $\mathcal{R} : \mathbb{T}^{N-1} \longrightarrow \mathbb{T}^{N-1}$, where*

$$\mathcal{R}(\varphi_1, \ldots, \varphi_{N-1}) = (\varphi_{N-1}, \ldots, \varphi_1), \quad t \longmapsto -t. \tag{23}$$

Proof. One can check that

$$\begin{aligned} G_i(\mathcal{R}\Phi) &= G_i(\varphi_{N-1}, \ldots, \varphi_1) \\ &= \sum_{j=1}^{[(N-1)/2]} K_j (g(\varphi_{-j}) - g(\varphi_j) - g(\varphi_{-(i+j)} - \varphi_{-i}) + g(\varphi_{-(i-j)} - \varphi_{-i})) \\ &= - \sum_{j=1}^{[(N-1)/2]} K_j (g(\varphi_j) - g(\varphi_{-j}) - g(\varphi_{(-i)+j} - \varphi_{-i}) + g(\varphi_{(-i)-j} - \varphi_{-i})) \\ &= -G_{-i}(\varphi_1, \ldots, \varphi_{N-1}) = -G_{N-i}(\Phi) \end{aligned}$$

for any $i = 1, \ldots, N-1$. This implies

$$(G_1(\mathcal{R}\Phi), \ldots, G_{N-1}(\mathcal{R}\Phi))^T = -\mathcal{R}(G_1(\Phi), \ldots, G_{N-1}(\Phi))^T. \qquad \blacksquare$$

We emphasize that the reversibility property is independent of the coupling function $g(x)$. The fixed subspace of the involution $\mathcal{R}$ is

$$\mathrm{Fix}\,\mathcal{R} = \{\Phi \in \mathbb{T}^{N-1} : \mathcal{R}\Phi = \Phi\} = \left\{ \Phi \in \mathbb{T}^{N-1} : \varphi_i = \varphi_{N-i},\ 1 \le i \le \left[\frac{N-1}{2}\right] \right\}.$$

Generically, the dimension of this set is $d(N) := \dim(\mathrm{Fix}\,\mathcal{R}) = N - 1 - [(N-1)/2] = [N/2]$. The subspace $\mathrm{Fix}\,\mathcal{R}$ can be used for describing the dynamical features of the system, because of the following properties:

- If some orbit intersects $\mathrm{Fix}\,\mathcal{R}$ at two points, then it is periodic, and it consists of two parts that are mapped into each other by the involution $\mathcal{R}$.
- Any nonperiodic trajectory can intersect $\mathrm{Fix}\,\mathcal{R}$ only once (in the opposite case this trajectory is periodic).
- If a reversible system has a sink or source equilibrium, then it does not belong to $\mathrm{Fix}\,\mathcal{R}$.
- If a reversible system has a sink (source) $\mathcal{M}$, then $\mathcal{R}\mathcal{M}$ is an equilibrium, and it is a source (sink).
- If a trajectory starts from a source and intersects $\mathrm{Fix}\,\mathcal{R}$, then it tends to a symmetry-related sink, and this trajectory is heteroclinic (as in Figures 3, 4, and 5). Note that the reversibility does not imply the existence of a trajectory that starts from a source and intersects with $\mathrm{Fix}\,\mathcal{R}$, i.e., the sink and the related source can be disconnected.

Since all trajectories that intersect $\mathrm{Fix}\,\mathcal{R}$ two times are time-periodic, it is instructive to consider the intersection of $\mathrm{Fix}\,\mathcal{R}$ with its evolution under the flow:

$$\mathcal{F}_t(\mathrm{Fix}\,\mathcal{R}) = \{\Phi(t) :\ \Phi(0) \in \mathrm{Fix}\,\mathcal{R}, t \in \mathbb{R}\}.$$

Reversible periodic trajectories appear for all points of the intersection $\mathrm{Fix}\,\mathcal{R} \cap \mathcal{F}_t(\mathrm{Fix}\,\mathcal{R})$. Since the dimension of $\mathcal{F}_t(\mathrm{Fix}\,\mathcal{R})$ is $d_t(N) := \dim(\mathcal{F}_t(\mathrm{Fix}\mathcal{R})) = [N/2] + 1$, according to the transversality theorem, the dimension of the intersection in $\mathbb{T}^{N-1}$ is generically

$$d^*(N) := \dim(\mathrm{Fix}\mathcal{R} \cap \mathcal{F}_t(\mathrm{Fix}\mathcal{R})) = d(N) + d_t(N) - (N-1) = \begin{cases} 1 & \text{when} \quad N \quad \text{is odd,} \\ 2 & \text{when} \quad N \quad \text{is even.} \end{cases}$$

Therefore, we generically expect that system (22) possesses one- or two-parametric families of periodic orbits, depending on the parity of the phase space dimension. Examples of such families will be described in the low-dimensional cases in section 5. In particular, for the cases $N = 3$ and $N = 4$, when the phase space of the reduced equation (22) is 2 and 3, respectively, the families of periodic orbits occupy open sets of the phase space forming the Hamiltonian-like domains filled with just periodic orbits. However, already for $N = 5$, when the phase space of (22) is four-dimensional, the families of periodic orbits do not occupy an open subset of the phase space but rather form two-dimensional invariant manifolds. As a result, other states appear such as quasi-periodic or chaotic.

The following proposition holds.

Proposition 4.2. *For $g'(0) \neq 0$ and for almost all skew-symmetric couplings K such that $K_j = -K_{-j}$, system (22) possesses the following dynamics:*

(A) *Families of periodic orbits in the vicinity of $\mathcal{M}_0$: There exists a one-parameter family of periodic solutions $\Phi_\sigma(t)$ in the neighborhood of $\mathcal{M}_0$ when N is odd and a two-parameter family $\Phi_{(\sigma_1,\sigma_2)}(t)$ of periodic solutions when N is even, with periods close to $2\pi/\Omega_m$, where $\Omega_m = 2g'(0)\sum_{j=1}^{[(N-1)/2]} K_j \sin(\frac{2mj\pi}{N})$.*

(B) *Dense set of invariant tori in the vicinity of $\mathcal{M}_0$: Under the nonresonance and nondegeneracy conditions* (b1) *and* (b2)*, given below, in any neighborhood of $\mathcal{M}_0$*

there exist analytic $[(N-1)/2]$-dimensional tori with conditionally-periodic motions with incommensurable frequencies close to $\Omega_1, \dots, \Omega_{[(N-1)/2]}$. The tori are invariant with respect to the flow and with respect to the reversibility transformation $\mathcal{R}$. Moreover, if U_ε is an ε-neighborhood of $\mathcal{M}_0$, then the Lebesgue measure of the invariant tori tends to the full measure of the neighborhood U_ε, as $\varepsilon \to 0$.

(b1) *Nonresonance: $(q,\Omega) = \sum_{m=1}^{[(N-1)/2]} q_m\Omega_m \neq 0$ is satisfied for all q with $|q| \le 2l+2$ and some $l \in \mathbb{N}$.*

(b2) *Nondegeneracy: The leading cubic terms (i.e., their imaginary parts) of the normal form are nondegenerate (equivalent to operator Γ in [60]).*

(C) *The statements* (A) *and* (B) *hold also for a neighborhood of $\mathcal{M}_{N/2}$ if N is even.*

(D) *Dissipative dynamics: The equilibrium $\mathcal{M}_k$, $k \neq 0$, is a sink if the condition*

$$\mathrm{Re}(\lambda_m(\mathcal{M}_k)) = \sum_{j=1}^{[(N-1)/2]} K_j\left(\eta_{kj} - \eta_{-kj}\right)\left(1 - \cos\left(\frac{2mj\pi}{N}\right)\right) < 0 \tag{24}$$

is satisfied for all $m = 1, \dots, N-1$. In this case $\mathcal{M}_{-k}$ is a source.

Proof. (A) The existence of families of periodic orbits can be shown using the Lyapunov center theorem for time-reversible systems [72, 26]. Using the skew-symmetry of the matrix K and expression (10), the eigenvalues of the synchronous state $\mathcal{M}_0$ are

$$\begin{aligned}\lambda_m(\mathcal{M}_0) = g'(0) &\sum_{j=1}^{[(N-1)/2]} (K_j + K_{-j})\left(1 - \cos\left(\frac{2mj\pi}{N}\right)\right)\\ &- \imath g'(0)\sum_{j=1}^{[(N-1)/2]} (K_j - K_{-j})\sin\left(\frac{2mj\pi}{N}\right)\\ &= -\imath 2g'(0)\sum_{j=1}^{[(N-1)/2]} K_j \sin\left(\frac{2mj\pi}{N}\right) =: \imath\Omega_m \end{aligned}\tag{25}$$

for any $m = 1, \dots, N-1$. Hence, $\lambda_{\pm m}(\mathcal{M}_0) = \pm\imath\Omega_m$, $m = 1, \dots, [(N-1)/2]$, and $\lambda_{N/2}(\mathcal{M}_0) = 0$ if N is even. It is easy to see from (25) that the following nonresonance conditions are satisfied for almost all values of K_j for $N \ge 5$ and for all values of K for $N = 3, 4$:

(i) all $\imath\Omega_m$ are simple eigenvalues of the Jacobian matrix $B(\mathcal{M}_0)$;

(ii) $\imath n\Omega_m$ are not eigenvalues of $B(\mathcal{M}_0)$ for all $n > 1$.

When N is odd, the conditions of [26, Theorem 1.1] are satisfied in the neighborhood of $\mathcal{M}_0 \in \mathrm{Fix}\,\mathcal{R}$. Therefore, there exists a one-parameter family of periodic solutions $\Phi_\sigma(t)$ of (22).

In the case of N even, Theorem 2.1 from [26] is applicable. In order to satisfy the conditions of this theorem, it is necessary to check that $\mathcal{R}$ is the identity transformation on $\ker(B(\mathcal{M}_0))$. Indeed, the eigenvector of the trivial eigenvalue $\lambda_{N/2}(\mathcal{M}_0) = 0$ is $v = (1,0,1,0,\dots,1,0,1)^T$, and $V_0 = \ker(B(\mathcal{M}_0)) = \mathrm{span}(v) = (\varphi,0,\varphi,0,\dots,\varphi,0,\varphi)$, $\varphi \in \mathbb{T}^1$, hence $\dim V_0 = 1$, and one can check that $\mathcal{R}v = v$. Therefore, as follows from [26, Theorem 2.1], there exists a two-parameter family of periodic orbits for even N in the vicinity of $\mathcal{M}_0$. The period of these solutions is close to $2\pi/\Omega_m$.

(B) The existence of dense families of quasi-periodic tori follows from the KAM theory for reversible systems [60, 48, 5, 16, 15, 14, 40]. Under the nonresonance and nondegeneracy conditions (b1) and (b2), the conditions of the theorem from [60] are satisfied. More specifically, the dimensions of tori are $(N-1)$ for odd N and $(N-2)$ for even N (in the notation of [60]: $m=(N-1)/2$, $k=0$ for odd, and $m=(N-2)$, $k=1$ for even dimensions).

(C) It is easy to check that the equilibrium $\mathcal{M}_{N/2}$ is neutral because $\eta_{N/2j}-\eta_{-N/2j}=0$ and, therefore, $\mathrm{Re}(\lambda_m(B(\mathcal{M}_{N/2})))=0$ for any m. Since $\mathcal{M}_{N/2}\in \mathrm{Fix}\,\mathcal{R}$, the same arguments as in (A) and (B) can be applied.

(D) We know that the system has equilibria $\mathcal{M}_k$ independently of system parameters and we can check the stability of these points using Proposition 3.3 and Corollary 3.4. In particular, the real parts of the eigenvalues of $\mathcal{M}_k$, $k\neq 0$, are

$$\mathrm{Re}(\lambda_m(\mathcal{M}_k)) = \sum_{j=1}^{[(N-1)/2]} K_j\left(\eta_{kj}-\eta_{-kj}\right)\left(1-\cos\left(\frac{2mj\pi}{N}\right)\right), \tag{26}$$

$m=1,\dots,N-1$. According to the time-reversal symmetry $\mathcal{R}$ the equilibrium $\mathcal{M}_{-k}$ is a source if $\mathcal{M}_k$ is a sink and vice versa. ■

Remark.

1. Condition (24) is only sufficient, and it can be weakened using the fact that the system can have other attractors/repellors except for $\mathcal{M}_k$.
2. The cases when $g(x)$ is odd or even can be special. One can see that condition (24) is not satisfied when the function $g(x)$ is odd. Also $\mathrm{Im}(\lambda_m(\mathcal{M}_0))=0$, $m=1,\dots,N-1$, when $g(x)$ is even. This implies that in this situation the origin is a degenerate saddle and the conservative region may shrink to a single point.
3. We note that the superposition of symmetries Z_N and $\mathcal{R}$ implies the existence of $N-1$ other reversal symmetries $\mathcal{R}_i$, $i=2,\dots,N$. Hence, there exist $N-1$ hyperplanes $\mathrm{Fix}\,\mathcal{R}_i=\gamma^i_{Z_N}\mathrm{Fix}\,\mathcal{R}_1$ that are fixed under the transformations $\mathcal{R}_i$, $i=2,\dots,N-1$. All $\mathrm{Fix}\,\mathcal{R}_i$ intersect in $\mathcal{M}_0$ if N is odd and they intersect along one-dimensional line $V_0\in\mathbb{T}^{N-1}$ when N is even.
4. If a periodic orbit intersects only one $\mathrm{Fix}\,\mathcal{R}_i$ in two points, then there are N Z_N-symmetry related periodic orbits. If a periodic orbit intersects at least two $\mathrm{Fix}\,\mathcal{R}_i$, then it intersects all of them. As will be illustrated later in section 5 for low-dimensional cases, the Hamiltonian-like dynamics is localized around the origin when N is odd and it translates along line V_0 when N is even. There is also the second "island" of Hamiltonian-like dynamics in the even-dimensional case around a neutral fixed point $\mathcal{M}_{N/2}$.

5. Bifurcation properties in low-dimensional systems.

In this section we study in detail the low-dimensional system (6)–(7) with specific coupling functions. Mostly, we consider the coupling function of Kuramoto–Sakaguchi type [57]

$$g(x) = -\sin(x-\alpha) \tag{27}$$

with a phase-shift parameter α. For $b=-a$, the system has time-reversal symmetry (23), which leads to the coexistence of Hamiltonian-like and dissipative dynamics as stated in

Proposition 4.2. The following results not only illustrate Proposition 4.2 but also provide more detailed information on the properties of both dissipative and Hamiltonian-like regions. In particular, we describe the structure of their boundaries and effects of the parameters on the size of the corresponding region.

We also note that for $a = b$ system (7) has the dihedral symmetry D_N. Moreover, system (7) with Kuramoto–Sakaguchi coupling (27) has additional symmetries Γ_1, Γ_2, and Γ_3 that are given by the actions

$$\gamma_1 : \ (\varphi_1, \dots, \varphi_{N-1}, a, b, \alpha, t) \longmapsto (\varphi_1, \dots, \varphi_{N-1}, -a, -b, \alpha, -t),$$
$$\gamma_2 : \ (\varphi_1, \dots, \varphi_{N-1}, a, b, \alpha, t) \longmapsto (-\varphi_1, \dots, -\varphi_{N-1}, a, b, -\alpha, -t),$$
$$\gamma_3 : \ (\varphi_1, \dots, \varphi_{N-1}, a, b, \alpha, t) \longmapsto (\varphi_1, \dots, \varphi_{N-1}, a, b, \alpha + \pi, -t).$$

5.1. Three coupled oscillators. The system of $N = 3$ identical oscillators with Kuramoto–Sakaguchi coupling function (27) written in phase differences has the following form:

$$\begin{aligned} \dot\varphi_1 &= -\sin(\varphi_1 - \alpha) - b\sin(\varphi_2 - \alpha) - b\sin(\varphi_1 + \alpha) - \sin(\varphi_1 - \varphi_2 + \alpha), \\ \dot\varphi_2 &= -\sin(\varphi_1 - \alpha) - b\sin(\varphi_2 - \alpha) - \sin(\varphi_2 + \alpha) - b\sin(\varphi_2 - \varphi_1 + \alpha). \end{aligned} \tag{28}$$

It possesses two parameters b and α, while we set the coupling parameter $a = 1$ without loss of generality.

It is known that the network of even three elements can have quite variative and complex dynamics depending of coupling structure (see, for example, [28, 29, 6, 47]). In the following, we describe dynamical properties of system (28) in detail. Particularly, Proposition 5.1 summarizes the coexistence of Hamiltonian-like and dissipative dynamics as well as a more detailed structure of the phase space for skew-symmetric coupling $b = -1$. The bifurcation diagram with respect to parameters α and b is shown in Figure 2(a), and typical phase portraits for different parameters are shown in Figures 3(a)–(l).

Symmetries and fixed points. The Z_3 symmetry in system (28) is generated by the action $\gamma_{Z_3} : \ (\varphi_1, \varphi_2) \longmapsto (-\varphi_2, \varphi_1 - \varphi_2)$. The origin $\mathcal{M}_0 = (0, 0)$ and the two points $\mathcal{M}_1 = (2\pi/3, 4\pi/3)$, $\mathcal{M}_2 = (4\pi/3, 2\pi/3)$ are equivariant under the action γ_{Z_3}. While the locations of these points do not depend on parameters, their stability does. In addition to the $\mathcal{M}_k$, the system has three Z_3-symmetric saddles. For $\alpha = 0$, the coordinates of these saddles are $(0, \pi)$, $(\pi, 0)$, and (π, π) (see Figure 3(a)), and they change with parameters. The saddles exist for all parameter values except for $\alpha = \pm\pi/2$. Simultaneous connections of stable and unstable one-dimensional manifolds of the three saddles create Z_3-heteroclinic cycles for some parameter values; see Figures 3(c), (f), (g), and (j).

Bifurcations of fixed points (see Figure 2(a)). As follows from Corollary 3.6 and condition (16), the Andronov–Hopf bifurcation lines for the points $\mathcal{M}_k$ are given by the expressions

$$H_k = \left\{ (\alpha, b) : \ b = -\frac{\cos(2k\pi/3 - \alpha)}{\cos(2k\pi/3 + \alpha)} \right\}, \quad k = 0, 1, 2.$$

In particular, the corresponding bifurcation line for the origin $\mathcal{M}_0$ is $b = -1$.

Z_3-symmetric transcritical bifurcations of the origin occur on the bifurcation lines $\alpha = \pm\pi/2$, where the second condition of (19) holds: $g'(0) = 0$. In this case, three symmetric saddle

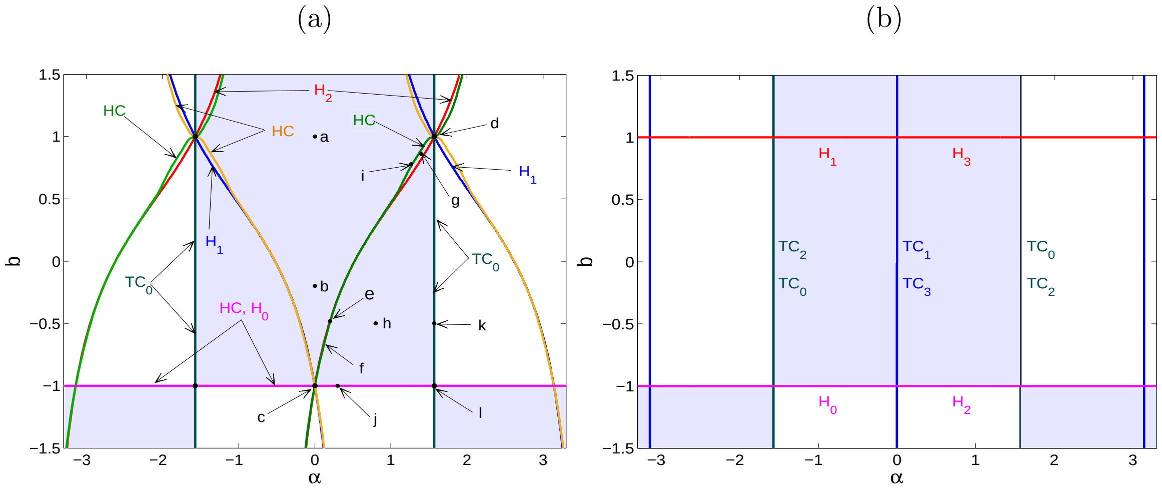

Figure 2. *Bifurcation diagrams in (α, b) bifurcation plane for three* (a) *and four* (b) *coupled oscillators. H_k: line of the Andronov–Hopf bifurcation of $\mathcal{M}_k$; TC_k: transcritical bifurcation of $\mathcal{M}_k$; HC: heteroclinic (saddle connection). Lines HC and H_2 (H_1) are located very close to each other; they intersect at $b \approx -0.4$ and partially merge in figure* (a). *The points* a–l *indicate parameter values, for which corresponding qualitatively different phase portraits are shown in Figure 3.* g *and* f *indicate upper and lower parts of the same HC line;* i *and* e *indicate upper and lower regions between H_2 and HC; c$(0, 1)$, d$(\pi/2, 1)$, l$(\pi/2, -1)$ are codimension-two bifurcation points;* j *belongs to H_0 between* c *and* l; k *belongs to TS_0 between* d *and* l. *Shaded regions show stability regions of the synchronous solution.*

points (Figures 3(a), (b)) approach the origin simultaneously and create a degenerate saddle at the bifurcation moment (Figures 3(d), (k)). Then the saddles pass the origin changing its stability.

Two heteroclinic bifurcation lines HC are very close to the Andronov–Hopf lines H_1 and H_2 of $\mathcal{M}_1$ and $\mathcal{M}_2$, respectively. HC and H lines intersect at the points $(\alpha, b) = (0, -1)$, $(\pm\pi/2, 1)$, $(\pm\pi/2, -1)$ and at the point where coordinate b is close to -0.4. The global HC bifurcation consists of three symmetric saddle connections and it creates stable (Figure 3(g)) or unstable (Figure 3(f)) heteroclinic cycles. This bifurcation leads to the appearance of a limit cycle with the same stability as the heteroclinic cycle (Figures 3(i), (e)). As a result, limit cycles appear at the H bifurcation and disappear in HC bifurcation (or vice versa). The third symmetric HC bifurcation line coincides with the H_0 line $b = -1$.

The system (28) is conservative at the codimension-two bifurcation points $(\alpha, b) = (0, -1)$ (Figure 3(c)) and $(\alpha, b) = (\pm\pi, -1)$. There, it has the first integral

$$I(\varphi_1, \varphi_2) = \cos\varphi_1 + \cos\varphi_2 + \cos(\varphi_1 - \varphi_2).$$

The system is also conservative when $(\alpha, b) = (\pi/2, 1)$ (Figure 3(d)).

The regions where the origin is stable consist of two parts: (1) $b > -1$, $\alpha \in (-\pi/2, \pi/2)$ and (2) $b < -1$, $\alpha \in (\pi/2, 3\pi/2)$ (gray in Figure 2(a)). The regions of the stability of $\mathcal{M}_k$, $k = 1, 2$, are located between two neighboring H_i lines and it has width π along the α-axis. In particular, the stability region for $\mathcal{M}_1$ is located between two (blue) bifurcation lines H_1 in Figure 2(a) and it satisfies the inequalities

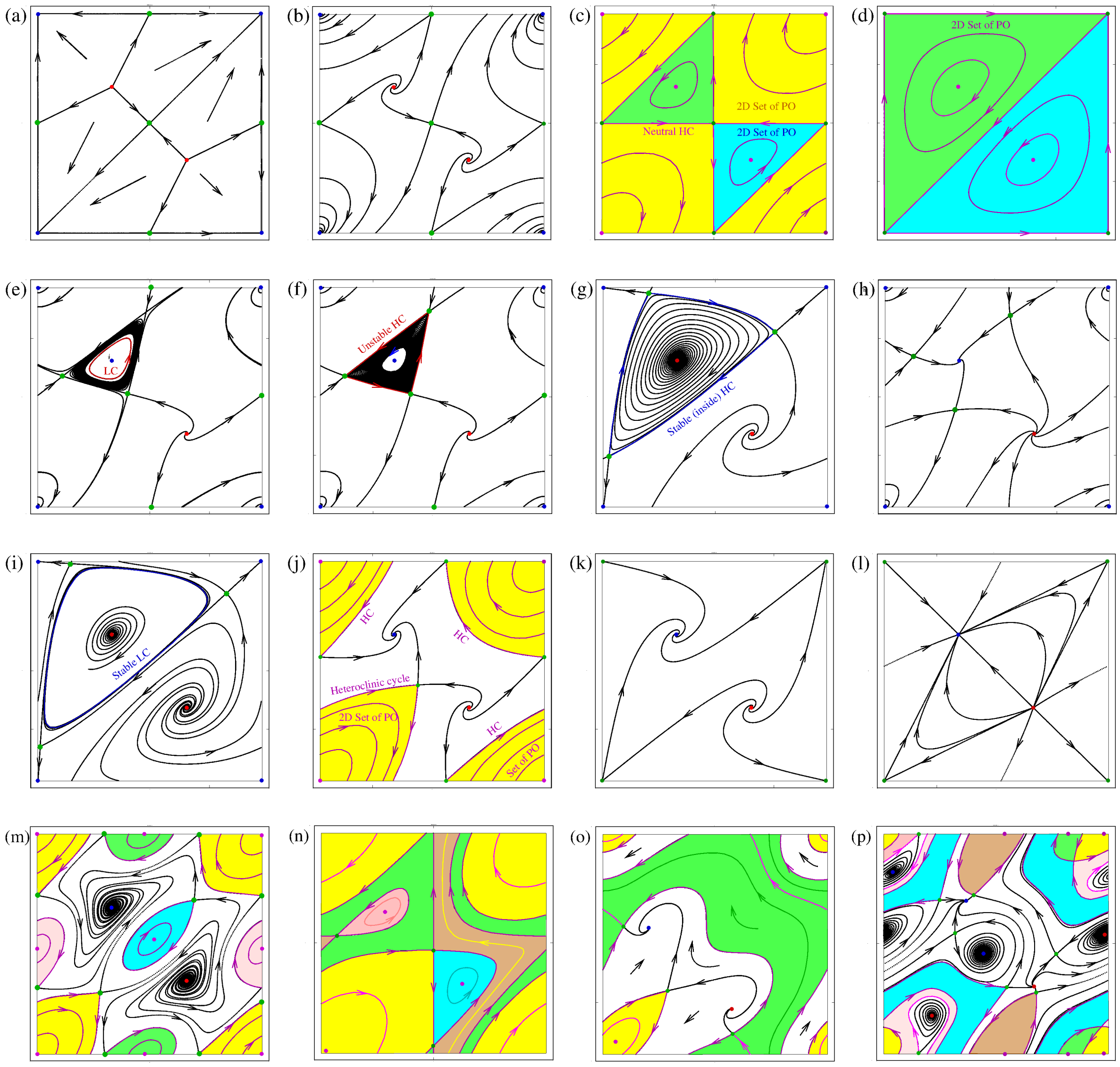

Figure 3. *Phase portraits for different parameter values for $N = 3$ coupled oscillators. Phase portraits in* (a)–(l) *correspond to system* (28) *and parameters from the points* a *to* l *in Figure* 2(a)*. For all figures in the bottom panel $b = -1$ and for* (m) $\alpha = 0.2$, $\Delta_1 = \Delta_2 = 0$, $p = 2$, *for* (n) $\alpha = 0$, $\Delta_1 = 0$, $\Delta_2 = 0.2$, $p = 0$, *for* (o) $\alpha = 0.2$, $\Delta_1 = -\Delta_2 = -0.6$, $p = 0.4$, *for* (p) $\alpha = 0.4$, $\Delta_1 = 0.1$, $\Delta_2 = 0.2$, $p = -0.9$. *Phase portraits* (m), (o), *and* (p) *correspond to the coupling function* (33) *with additional second harmonic term;* (n)–(p) *are phase portraits for different natural frequencies of the oscillators. Colored areas indicate Hamiltonian-like regions in the phase space that are filled with neutrally stable limit cycles. Colors for fixed points indicate as follows: red—source; blue—sink; green—saddle; magenta—center; dark green—degenerate saddle. Stable limit cycles are shown in blue, unstable in red.*

$$\arctan\left(\frac{1+b}{\sqrt{3}(1-b)}\right) + 2n\pi < \alpha < \arctan\left(\frac{1+b}{\sqrt{3}(1-b)}\right) + (2n+1)\pi, \qquad n \in \mathbb{Z}.$$

The case $b = -1$ (α arbitrary) is especially interesting for us. In this case, the system possesses the time-reversal symmetry $\mathcal{R}$ presented by the action (23). The line $\mathrm{Fix}\,\mathcal{R}$: $\{(\varphi_1, \varphi_2),\, \varphi_1 = \varphi_2\}$ is fixed under this symmetry. The superposition of Z_3 and $\mathcal{R}$ gives two other reversible symmetries with the corresponding fixed subspaces $\varphi_1 = 0$ and $\varphi_2 = 0$. As a result, the system has Hamiltonian-like and dissipative regions that coexist in the phase space, yellow and white regions, respectively, in Figure 3(j). The following proposition rigorously states that the phase portrait shown in Figure 3(j) holds qualitatively for almost all values of the parameter α when $b = -1$.

Proposition 5.1. *For $b = -1$ and $\alpha \notin \{0, \pm\pi/2, \pi\}$, system (28) possesses the following dynamics in the phase space:*

(A) *Hamiltonian-like region: There exists a region in the phase space which contains the origin $\mathcal{M}_0$ and which is foliated by a one-parametric family of periodic orbits. This region is bounded by a Z_3-equivariant heteroclinic cycle consisting of three saddle points and connecting one-dimensional invariant manifolds of these saddles. The corresponding saddle points belong to the fixed subspace of the reversibility symmetry $\mathrm{Fix}\,\mathcal{R}$ or one of its symmetry images under the action of Z_3.*

(B) *Dissipative region: The points $\mathcal{M}_1$ and $\mathcal{M}_2$ are sink and source, respectively. That is, there exist neighborhoods of the points $\mathcal{M}_1$ (resp., $\mathcal{M}_2$) such that all orbits starting from these neighborhoods are asymptotically attracted to $\mathcal{M}_1$ (resp., repelled from $\mathcal{M}_2$).*

Proof. (A) Proposition 4.2 implies that system (28) has a one-parameter family $\Phi_\sigma(t)$ of periodic solutions with periods near $2\pi/\Omega_1$ where $\Phi_0(t) = \mathcal{M}_0$ and the parameter σ varies along $\mathrm{Fix}\,\mathcal{R}$. Hence, a neighborhood of $\mathcal{M}_0$ is foliated by periodic orbits.

Let us now show that the maximal region $\mathcal{D}_0$ containing the set of neutral periodic orbits is bounded by the heteroclinic cycle. It is known that the boundary of an invariant region is flow-invariant. For our two-dimensional system, three types of invariant sets are possible: a limit cycle, a homoclinic cycle, and a heteroclinic cycle. A limit cycle is impossible because it must be neutral from the inside (it borders neutral periodic orbits), and it is neutral from the outside as well, since any trajectory in its small neighborhood intersects $\mathrm{Fix}\,\mathcal{R}$ twice and is, therefore, periodic. Hence the assumed bounding periodic orbit is neutral and is internal with respect to $\mathcal{D}_0$. A homoclinic cycle cannot be a border of $\mathcal{D}_0$, since, according to Z_3 symmetry, there are three such homoclinic loops that are connected to three different saddles S_i and contain the same neutral fixed point $\mathcal{M}_0$. Hence these homoclinic orbits must intersect each other, leading to a contradiction. Therefore, a Z_3-symmetric heteroclinic cycle is the only possible border for $\mathcal{D}_0$. More specifically, it consists of three saddles, $S_1\,(\widetilde{\varphi}, \widetilde{\varphi}) \in \mathrm{Fix}\,\mathcal{R}_1$, $S_2\,(-\widetilde{\varphi}, 0) \in \mathrm{Fix}\,\mathcal{R}_2$, $S_3\,(0, -\widetilde{\varphi}) \in \mathrm{Fix}\,\mathcal{R}_3$, where $\widetilde{\varphi} = \pi\text{-}2\alpha$, $\mathrm{Fix}\,\mathcal{R}_i = \tilde{\gamma}_{Z_3}^{i-1}\mathrm{Fix}\,\mathcal{R}$, $i = 1, 2, 3$, and of three one-dimensional invariant manifolds of these saddles.

(B) The eigenvalues of $\mathcal{M}_1$ are $-\frac{3\sqrt{3}}{2}\sin\alpha \pm \imath\frac{\sqrt{3}}{2}\cos\alpha$; hence, for $\alpha \notin \{0, \pi\}$, $\mathcal{M}_1$ is either a source or sink. ■

Our numerical observations (using numerical integration, software AUTO [22], as well as DsTool [8]) indicate that the dissipative region extends to $\mathbb{T}^2 \setminus \mathcal{D}_0$.

We note that system (28) also has another time-reversal symmetry $\mathcal{R}' : (\varphi_1, \varphi_2) \longmapsto (-\varphi_2, -\varphi_1)$ at the codimension-two points $(\alpha, b) = (0, -1)$ and $(\alpha, b) = (\pm\pi/2, 1)$ (Figures 3(c) and (d) correspondingly). The fixed subspace of $\mathcal{R}'$ is $\mathrm{Fix}\,\mathcal{R}' = \{(\varphi_1, -\varphi_1), \varphi_1 \in \mathbb{T}^1\}$. A further time-reversal symmetry $\mathcal{R}'' : (\varphi_1, \varphi_2) \longmapsto (-\varphi_1, -\varphi_2)$ exists when $\alpha = \pm\pi/2$ for any parameter b (Figures 3(d), (k) and (l)). $\mathrm{Fix}\,\mathcal{R}''$ in this situation consists of only two points $(\varphi_1, \varphi_2) = (0, 0)$ and $(\varphi_1, \varphi_2) = (\pi, \pi)$ in contrast to the previous case where $\mathrm{Fix}\mathcal{R}'$ is a one-dimensional line.

5.2. Four coupled oscillators. System (7) of $N = 4$ identical oscillators is three-dimensional for the phase differences $(\varphi_1, \varphi_2, \varphi_3)$:

$$\dot{\varphi}_i = g(\varphi_1) - g(\varphi_{i+1} - \varphi_i) + b(g(\varphi_3) - g(\varphi_{i+3} - \varphi_i)), \quad i = 1, 2, 3, \tag{29}$$

where $g(x) = -\sin(x - \alpha)$. Here we also set $a = 1$ without loss of generality. Apart from the synchronous solution $\mathcal{M}_0$ at the origin, system (29) possesses the equilibria $\mathcal{M}_1 = (\pi/2, \pi, 3\pi/2)$, $\mathcal{M}_2 = (\pi, 0, \pi)$, and $\mathcal{M}_3 = (3\pi/2, \pi, \pi/2)$.

The bifurcation diagram in the parameter plane (α, b) for $N = 4$ is shown in Figure 2(b), where Andronov–Hopf (H) and transcritical (TC) bifurcation lines of the rotating waves are plotted. The stability region for the origin is the same as in the case of three oscillators (shaded). The stability region of the point $\mathcal{M}_2$ coincides with the instability region of the origin. Stability regions of two points $\mathcal{M}_1$ and $\mathcal{M}_3$ are also complementary to each other and are bounded by the lines $\alpha = 0$, $\alpha = \pi$, and $b = 1$.

It is interesting to note that the system is conservative at the codimension-two points $(\alpha, b) = (0, -1)$ and $(\alpha, b) = (\pi, -1)$ with the first integrals $I_1(\varphi_1, \varphi_2, \varphi_3) = \varphi_1 - \varphi_2 + \varphi_3$ and $I_2(\varphi_1, \varphi_2, \varphi_3) = \cos(\varphi_1) + \cos(\varphi_1 - \varphi_2) + \cos(\varphi_2 - \varphi_3) + \cos(\varphi_3)$.

The case of skew-symmetric coupling $b = -1$ leads to the emergence of coexisting Hamiltonian-like and dissipative dynamics. The following proposition describes it in more detail.

Proposition 5.2. *For $b = -1$ and $\alpha \notin \{0, \pm\pi/2, \pm\pi\}$ system (29) possesses the following dynamics in the phase space:*

(A) *Hamiltonian-like region: There exist neighborhoods of the equilibria $\mathcal{M}_0$ and $\mathcal{M}_2$ which are foliated by two-parametric families of periodic orbits.*

(B) *Dissipative region: The equilibrium $\mathcal{M}_1$ is either a sink or a source. That is, there exists a neighborhood of the point $\mathcal{M}_1$, such that all orbits starting from this neighborhood are asymptotically attracted to $\mathcal{M}_1$ (resp., repelled). The equilibrium $\mathcal{M}_3$ has complementary stability properties.*

Proof. The proof follows from Proposition 4.2 with the following specific remarks: (A) According to (10), the eigenvalues of the origin are $\lambda_{1,3}(\mathcal{M}_0) = \pm\imath\Omega_1 = \pm\imath 2\cos(\alpha)$ and $\lambda_2 = 0$. For $\alpha \neq \pm\pi/2$, it holds that $\Omega_1 \neq 0$.

(B) We note that the Hamiltonian-like regions around $\mathcal{M}_0$ and $\mathcal{M}_2$ shrink to points when $|\alpha|$ approach $\pi/2$. ■

The following observations provide more details and complete the global picture of the dynamics in the phase space for $b = -1$; they are also summarized in Figure 4. We note that the superposition of Z_4 and $\mathcal{R}$ gives another time-reversal symmetry $\mathcal{R}'$ with

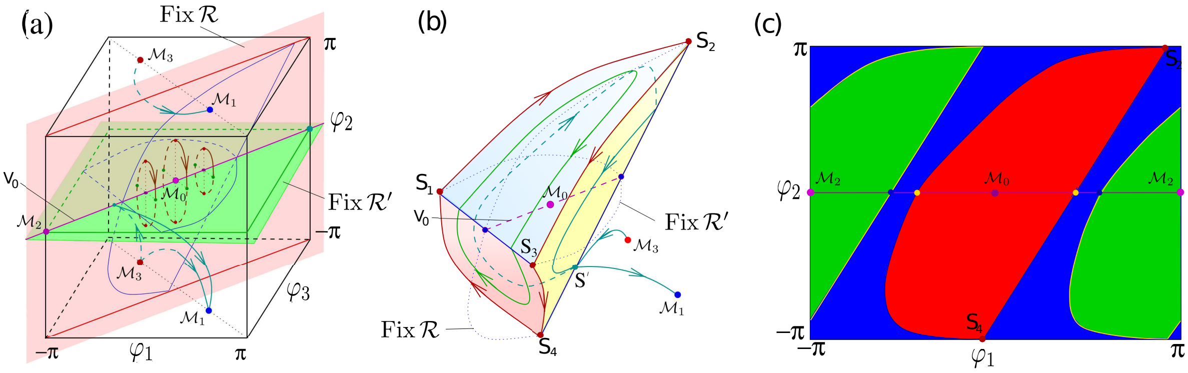

Figure 4. (a) *Structure of the phase space of the system of four coupled oscillators* (29) *for* $b = -a = -1$ *and* $\alpha \in (0, \pi/2)$. (b) *Hamiltonian-like region* $\mathcal{D}$ *filled by a two-parametric family of periodic orbits and bounded by a surface of heteroclinic cycles.* (c) *Fixed subspace for the time-reversibility transformation* $\operatorname{Fix}\mathcal{R}$ *as a Poincaré section for the system when* $\alpha = 0.2$. *Blue region indicates the intersection of* $\operatorname{Fix}\mathcal{R}$ *with the attraction basin of the rotating wave* $\mathcal{M}_1$ *(heteroclinic trajectories start at* $\mathcal{M}_3$, *intersect* $\operatorname{Fix}\mathcal{R}$, *and converge to* $\mathcal{M}_1$*). Red and green regions indicate families of nonisolated periodic orbits that intersect* $\operatorname{Fix}\mathcal{R}$ *transversally in neighborhoods of* $\mathcal{M}_0$ *and* $\mathcal{M}_2$*, respectively.*

$\operatorname{Fix}\mathcal{R}'$: $\{(\varphi_1, \varphi_2, \varphi_3) : \varphi_2 = 0\}$. The intersection of the planes $\operatorname{Fix}\mathcal{R}$ and $\operatorname{Fix}\mathcal{R}'$ gives the one-dimensional flow-invariant subspace $V_0 = \operatorname{Fix}\mathcal{R} \cap \operatorname{Fix}\mathcal{R}' = \{(\varphi, 0, \varphi),\ \varphi \in \mathbb{T}^1\} = \operatorname{span} v$, where $v = (1, 0, 1)$ is an eigenvector corresponding to the eigenvalue $\lambda_2 = 0$ of the equilibrium $\mathcal{M}_0$. It is easy to check that the whole line V_0 is filled with equilibria. The equilibrium $\mathcal{M}_2$ belongs also to subspace V_0. The equilibria in $V_0 \bigcap (\mathcal{D}_0 \bigcup \mathcal{D}_0')$ are neutral in the directions transverse to V_0 and they are saddles otherwise, outside of the conservative regions. Each periodic trajectory rotates around V_0 and it has two intersections with invariant plane $\operatorname{Fix}\mathcal{R}$ at points $(\overline{\varphi}_1, \overline{\varphi}_2, \overline{\varphi}_1)$, $(\overline{\varphi}_1 - \overline{\varphi}_2, -\overline{\varphi}_1, \overline{\varphi}_1 - \overline{\varphi}_2)$ and two corresponding intersections with $\operatorname{Fix}\mathcal{R}'$ at $(-\overline{\varphi}_1, 0, \overline{\varphi}_2 - \overline{\varphi}_1)$, $(\overline{\varphi}_2 - \overline{\varphi}_1, 0, -\overline{\varphi}_1)$. One can check that the plane $\operatorname{Fix}\mathcal{R}$ contains two lines of nonisolated fixed points $\varphi_2 = 2(\varphi_1 + \alpha) \pm \pi$ (or, equivalently, this is one line in $\mathbb{T}^2$ with rotation number 1:2). Each fixed point of the line is a degenerate saddle, it is neutral along the line, and it has attractive and repulsive one-dimensional invariant manifolds in directions transversal to the line. According to the rotational symmetry, another invariant plane $\operatorname{Fix}\mathcal{R}'$ also has one-parametric lines of degenerate saddles defined by the expression $\varphi_3 = -\varphi_1 + 2\alpha \pm \pi$. Fixed points on the intersection of the above mentioned line with V_0 have all zero eigenvalues. There are four such points with coordinates $(\pm\pi \pm \alpha, 0, \pm\pi \pm \alpha)$ that are on the boundary between the conservative and the dissipative parts (Figure 4).

The one-parametric family of the invariant one-dimensional manifolds of saddles form a two-dimensional surface (tube), which is the boundary between the Hamiltonian-like region $\mathcal{D}_0$ ($\mathcal{D}_0'$) and the dissipative region. The whole separatrix surface consists of heteroclinic cycles that connect two degenerate saddles of the same invariant line. There are also heteroclinic orbits that connect the saddle of the invariant line and the sink $\mathcal{M}_1$ (or the source $\mathcal{M}_3$).

5.3. Five coupled oscillators. In the case of five coupled oscillators (6) with nearest-neighbor coupling ($l = 1$) and coupling function (27), the situation is more complicated, since the phase space is four-dimensional, and we are not able to give a complete description of the

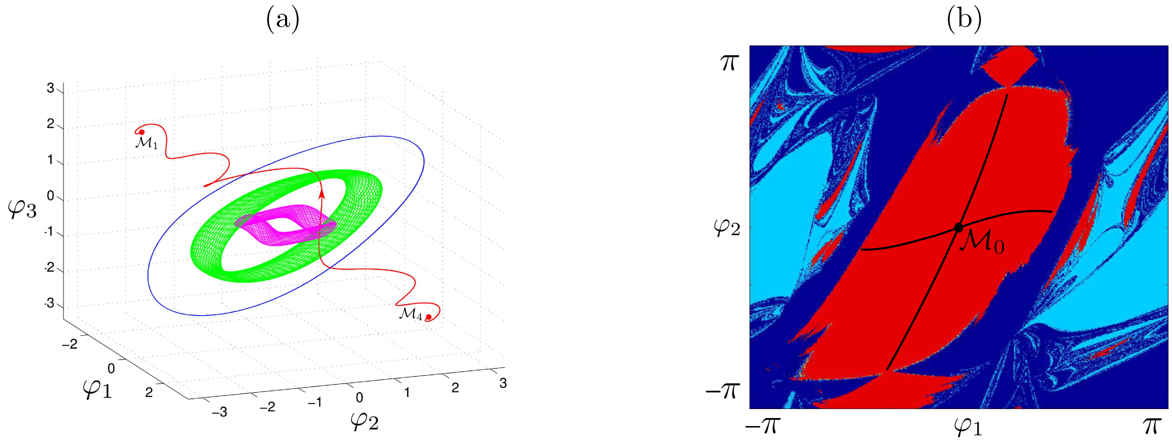

Figure 5. (a) *Trajectories of* (6) *for* $N = 5$ *and* $\alpha = 0.2$. *Blue trajectory is periodic; green and magenta are quasi-periodic with different amplitude; red trajectory is heteroclinic and connects the repeller* $\mathcal{M}_4$ *with the attracting equilibrium* $\mathcal{M}_1$. *The first three trajectories belong to the Hamiltonian-like part of the system, while the last one belongs to the dissipative part.* (b) *Different domains of the fixed point subspace of the involution* $\mathcal{R}$: *red—Hamiltonian-like region, where all Lyapunov exponents are close to zero; light and dark blue—attraction basin of one of the asymptotically stable rotating waves. Black lines correspond to the families of periodic orbits.*

phase space structure as in the case of $N \leq 4$. Nevertheless, one can illustrate the coexistence of dissipative and Hamiltonian-like regions that are densely filled with two-dimensional tori and families of periodic orbits. Figure 5(a) shows different trajectories belonging to the dissipative domain (heteroclinic orbit in red) and Hamiltonian-like (tori in green and magenta, as well as a periodic orbit in blue).

The following result follows from Proposition 4.2.

Corollary 5.3. *For* $b = -1$ *and* $\alpha \notin \{0, \pm\pi/2, \pm\pi\}$, *system* (6) *of* $N = 5$ *oscillators with coupling function* (27) *possesses the following dynamics in the phase space:*

(A) *Hamiltonian-like region:* (i) *In a neighborhood of* $\mathcal{M}_0$ *there exists a one-parameter family of periodic solutions.* (ii) *In any neighborhood of* $\mathcal{M}_0$ *there exists an analytic two-dimensional torus, which is invariant with respect to the flow and with respect to the reversibility transformation* $\mathcal{R}$. *Moreover, if* U_ε *is an* ε*-neighborhood of* $\mathcal{M}_0$, *then the Lebesgue measure of the invariant tori tends to the full measure of the neighborhood* U_ε, *as* $\varepsilon \to 0$.

(B) *Dissipative region: For* $0 < \alpha < \pi$, *the rotating waves* $\mathcal{M}_1$, $\mathcal{M}_2$ *are sinks and* $\mathcal{M}_3$, $\mathcal{M}_4$ *are sources. For* $-\pi < \alpha < 0$, *the stability is inverse, i.e.,* $\mathcal{M}_1$, $\mathcal{M}_2$ *are sources and* $\mathcal{M}_3$, $\mathcal{M}_4$ *are sinks.*

In Figure 5(b) we illustrate numerically the dynamics using the two-dimensional fixed point subspace of the involution $\mathcal{R}$:

$$\operatorname{Fix}\mathcal{R} = \{(\varphi_1, \varphi_2, \varphi_3, \varphi_4) : \varphi_1 = \varphi_4, \varphi_2 = \varphi_3\}.$$

The red domain in Figure 5(b) indicates a Hamiltonian-like region and blue the dissipative one. In particular the red domain corresponds to the points, which lead to the orbits with all four Lyapunov exponents close to zero (less than 10^{-4} in absolute value). The blue domain belongs to the attraction basin of one of the rotating waves: light blue to $\mathcal{M}_2$ and dark blue to $\mathcal{M}_1$. Black lines in Figure 5(b) correspond to one-parametric families of periodic orbits.

6. Nonidentical oscillators.

6.1. Divergence-free dynamics. We have shown that system (5) is Hamiltonian-like in the whole phase space for three and four oscillators when coupling function $g(x) = -\sin x$ and $a = -b$. The system has N neutral rotating wave points $\mathcal{M}_k$, saddles, heteroclinic structures, continuous sets of periodic orbits (as shown in Figure 3(c) for three oscillators), and quasi-periodic or chaotic trajectories (for higher dimensions). In such a case, the vector field has zero divergence even for arbitrary frequency differences Δ_i. The following proposition holds.

Proposition 6.1. (A) *The system* (5) *with arbitrary frequency differences* Δ_i, $i = 1, \dots, N-1$, *skew-symmetric coupling* $K_{-j} = -K_j$, *and odd coupling function* $g(x)$ *is divergence free.*

(B) *The system* (5) *with arbitrary frequency differences* Δ_i, $i = 1, \dots, N-1$, *symmetric coupling* $K_{-j} = K_j$, *and even coupling function* $g(x)$ *is divergence free.*

Proof. We give the proof for case (A), since case (B) is analogous.

$$\begin{aligned}
\operatorname{div} G(\Phi) &= \sum_{i=1}^{N-1} \frac{\partial \dot\varphi_i}{\partial \varphi_i} = \sum_{i=1}^{[(N-1)/2]} K_i(g'(\varphi_i) - g'(\varphi_{-i})) \\
&\quad + \sum_{i=1}^{N-1} \left(\sum_{j=1}^{[(N-1)/2]} K_j(g'(\varphi_{i+j} - \varphi_i) - g'(\varphi_{i-j} - \varphi_i)) \right) \\
&= \sum_{j=1}^{[(N-1)/2]} K_j \left(\sum_{i=0}^{N-1} (g'(\varphi_{i+j} - \varphi_i) - g'(\varphi_{i-j} - \varphi_i)) \right) \\
&= \sum_{j=1}^{[(N-1)/2]} K_j \left(\sum_{i=0}^{N-1} (g'(\varphi_{i+j} - \varphi_i) - g'(\varphi_i - \varphi_{i+j})) \right) = 0,
\end{aligned}$$

since $g'(x) = g'(-x)$ is implied by $g(x) = -g(-x)$. ■

Remark. We remark that a system of Kuramoto–Sakaguchi oscillators with the phase shift $\alpha = \pi/2$ is a particular situation of case (B) of Proposition 6.1.

Proposition 6.2. *The system* (22) *with nearest-neighbor coupling*

$$\dot\varphi_i = K_1(g(\varphi_1) - g(\varphi_{-1}) - g(\varphi_{i+1} - \varphi_i) + g(\varphi_{i-1} - \varphi_i))$$

and odd coupling function $g(\varphi)$ *has the first integral*

$$I_1(\varphi_1, \dots, \varphi_{N-1}) = \sum_{i=0}^{N-1} h(\varphi_i - \varphi_{i+1}),$$

where $h'(\varphi) = g(\varphi)$, $\varphi_N = \varphi_0 = 0$. *We note that* $h(\varphi)$ *is even.*

Proposition 6.3. *Consider the system (22) with even oscillator number and odd coupling function $g(\varphi)$ with skew-symmetric coupling matrix ($K_j = -K_{-j}$) and $K_j = 0$ for even j, i.e., oscillators are coupled with the nearest neighbors, third neighbor, fifth neighbor, etc. This system has the first integral*

$$I_2(\varphi_1, \ldots, \varphi_{N-1}) = \sum_{i=1}^{N-1} (-1)^{i-1} \varphi_i.$$

6.2. Pairwise equidistant natural frequencies and reversibility. In this section we show that the general system (5) can have the reversibility property when the coupling is skew-symmetric and the frequencies are not identical but satisfy a particular relation. System (5) for skew-symmetric coupling can be written as

$$\dot{\varphi}_i = \Delta_i + \sum_{j=1}^{[(N-1)/2]} K_j (g(\varphi_j) - g(\varphi_{-j}) - g(\varphi_{i+j} - \varphi_i) + g(\varphi_{i-j} - \varphi_i)), \tag{30}$$

where $i = 1, \ldots, N-1$; see also (22).

Proposition 6.4. *System (30) is time-reversible with the involution $\mathcal{R}$ determined by (23) if and only if the following relation between the frequency differences holds:*

$$\Delta_{N-i} = -\Delta_i, \quad i = 1, \ldots, [N/2]. \tag{31}$$

Proof. We rewrite system (30) as

$$\dot{\varphi}_i = \tilde{G}_i(\varphi_1, \ldots, \varphi_{N-1}) = \Delta_i + G_i(\varphi_1, \ldots, \varphi_{N-1}), \quad i = 1, \ldots, N-1. \tag{32}$$

It holds that

$$\tilde{G}_i(\mathcal{R}\Phi) = \Delta_i + G_i(\mathcal{R}\Phi) = -(-\Delta_i + G_{N-i}(\Phi))$$

and

$$-\tilde{G}_{N-i}(\Phi) = -(\Delta_{N-i} + G_{N-i}(\Phi)).$$

■

Remark. Note that (31) and, hence, conditions of Proposition 6.4 hold for the particular case of equally distributed frequencies $\omega_j = \omega_0 + hj$ in the case of an odd number N of oscillators.

In this case it is easy to see that the reversibility condition (23) is satisfied if and only if (31) holds, which corresponds to pairwise equidistant distribution of frequency pairs around the frequency of the first oscillator: $(\omega_{i+1} + \omega_{N-i+1})/2 = \omega_1$. We recall that $\Delta_{N/2} = 0$ when N is even.

As a result of Proposition 6.4, the Hamiltonian-like dynamics appears in systems of non-identical oscillators that satisfy relation (31). Indeed, at least for small deviations Δ from zero, the families of periodic orbits that are mentioned in statement (A) of Proposition 4.2 persist, since they appear due to the generic intersection of $\mathcal{F}_t(\operatorname{Fix}\mathcal{R})$ and $\operatorname{Fix}\mathcal{R}$. The dissipative equilibria remain also dissipative under small perturbations.

6.3. Nonhomotopic to zero Hamiltonian-like part. A Hamiltonian-like dynamics of (30) that is nonhomotopic to zero is possible when $|\Delta_i|$ are large enough. An example is shown in Figure 3(o) for three oscillators, where such a region is foliated by periodic trajectories that are nonhomotopic to zero. There might be a coexistence of the regions with homotopic to zero periodic orbits with another region filled with nonhomotopic to zero periodic orbits; see the yellow and green regions in Figure 3(o). The coexistence of many regions of two types is also possible, as shown in Figure 3(p) for $N = 3$ and the coupling function

$$g(x) = -\sin(x - \alpha) + p\sin(2x) \tag{33}$$

with an additional parameter p. Increasing frequency differences $|\Delta_i|$ from zero leads to a sequence of the disappearance of equilibria via local bifurcations. The homotopic to zero Hamiltonian-like part of the dynamics disappears together with the disappearance of the equilibrium within $\mathrm{Fix}\,\mathcal{R}$. Then, a possible Hamiltonian-like part can consist only of nonhomotopic to zero nonisolated orbits. Similar situations were observed for other systems in [69] and [68]. From this point of view, it is instructive to give conditions when the system does not possess equilibria.

Proposition 6.5. *System (30) does not have fixed points when one of the following conditions is satisfied:*

$$\min_{x\in\mathbb{T}^1} g(x) > -4[(N-1)/2]\min_i |\Delta_i|$$

or

$$\max_{x\in\mathbb{T}^1} g(x) < -4[(N-1)/2]\max_i |\Delta_i|.$$

Proof. The proof follows from the conditions $\Delta_i + \widetilde{G}_i(\Phi) > 0$ (< 0) for $i = 1, \dots, [N/2]$. Note that the conditions of this proposition are satisfied when the frequency differences are large enough. ■

7. Large system ($N \to \infty$) and nonlinear Schrödinger amplitude equation for skew-symmetric coupling. In this section we consider the dynamics in a neighborhood of the synchronous solution $\theta_i = \theta$ in the case of very large chains (i.e., $N \gg 1$) of identical oscillators, where each oscillator is coupled with a finite number $2l$ of its neighbors:

$$\dot\theta_i = \omega + \sum_{j=-l}^{l} K_j\, g(\theta_i - \theta_{i+j}), \quad i = 1, \dots, N, \tag{34}$$

and a *skew-symmetric* coupling matrix K, i.e., $K_j = -K_{-j}$, $j = 1, \dots, l$. The subscripts are taken modulo N, i.e., the system possesses the ring structure. For this case we will highlight once again that the dynamics behaves reversible, i.e., Hamiltonian like.

Using the "co-rotating" coordinates $\psi_i = \theta_i - \big(\omega + g(0)\sum_{-l}^{l} K_j\big)t$, system (34) reduces to

$$\dot\psi_i = \sum_{j=-l}^{l} K_j\, f(\psi_i - \psi_{i+j}) \tag{35}$$

with $f(x) = g(x) - g(0)$. Since $f(0) = 0$, the one-dimensional invariant synchronization manifold

$$\mathcal{S} = \{ (\psi_1, \dots, \psi_N) \, : \, \psi_i = \psi, \, i = 1, \dots, N \}$$

consists of equilibria $\psi_i = \psi = \text{const}$, which are related to each other by the phase-shift symmetry. Hence, the equilibria have neutral stability along the manifold and the same stability properties in the transverse directions to the manifold. Therefore, in order to study the dynamics in the neighborhood of a synchronous solution, it is enough to consider the neighborhood of the origin $\psi_i = 0$, $i = 1, \dots, N$. Note that in this section we do not write the system for phase differences (5) but work directly with (35). This will result in the persistence of the phase-shift symmetry in the obtained amplitude equations.

Expanding function $f(x)$ in Taylor series, we rewrite system (35) as follows:

$$\text{(36)} \quad \dot{\psi}_i = \sum_{j=-l}^{l} Q_j \psi_{i+j} + \frac{f''(0)}{2f'(0)} \sum_{j=-l}^{l} Q_j (\psi_i - \psi_{i+j})^2 + \frac{f'''(0)}{6f'(0)} \sum_{j=-l}^{l} Q_j (\psi_i - \psi_{i+j})^3 + O(\|\psi\|^4),$$

$$\text{where } Q_j = -K_j f'(0) \text{ for } j = -l, \dots, l, \; j \neq 0, \quad \text{and } Q_0 = f'(0) \sum_{j=-l, j\neq 0}^{l} K_j.$$

The Jacobian matrix Q is circulant and, similarly to (10), its eigenvalues are given by $\lambda_m(Q) = \sum_{-l}^{l} Q_j \mathrm{e}^{\imath 2\pi jm/N}$ for $m = 1, \dots, N$. In the limit of large N, the spectrum can be approximated by the *asymptotic continuous spectrum* [78, 79] via

(37)
$$\lambda(\phi) = \sum_{j=-l}^{l} \mathrm{e}^{\imath j\phi} Q_j = Q_0 + \sum_{j=1}^{l} \Big((Q_j + Q_{-j}) \cos(j\phi) + \imath (Q_j - Q_{-j}) \sin(j\phi) \Big), \quad \phi \in [0, 2\pi].$$

The function $\phi \mapsto \lambda(\phi)$, $\phi \in [0, 2\pi]$ presents a closed curve in the complex plane $\mathbb{C}$. Using the definition of Q_j with skew-symmetric coupling $K_{-j} = -K_j \in \mathbb{R}$, we obtain

$$\lambda(\phi) = \imath \, 2 \sum_{j=1}^{l} Q_j \sin(j\phi) = \imath \, \widetilde{\omega}(\phi) \quad \text{with } \widetilde{\omega}(\phi) \in \mathbb{R}.$$

Hence, the whole spectrum lies in the interval $[-\imath \max_\phi \widetilde{\omega}(\phi), \imath \max_\phi \widetilde{\omega}(\phi)] \subset \imath \, \mathbb{R}$.

The following result states that small-amplitude modulations of a basic spatially periodic pattern $\mathrm{e}^{\imath \phi_0 k}$ are governed by a nonlinear Schrödinger equation with suitable boundary conditions to guarantee the correct periodicity for the chain. Assuming that the coupling function has a *cubic nonlinearity* (i.e., $g''(0) = 0$) the approach in [35], adapted to the spatially discrete case as in [25, 78], yields the following statement.

Theorem 7.1. *Assume that system (36) satisfies the following conditions:*

(1) *the coupling matrix is skew-symmetric :* $Q_{-j} = -Q_j$*;*
(2) *there exists* $\phi_0 = 2\pi \frac{p}{q} \neq 0$ *with* $p, q \in \mathbb{N}$ *coprime,* $\omega_0 := \widetilde{\omega}(\phi_0) \neq 0$*, and* $\widetilde{\omega}''(\phi_0) \neq 0$*;*
(3) *the coupling function has a cubic nonlinearity at* $\theta = 0$*, i.e.,* $g''(0) = 0$*;*
(4) *the nonresonance condition* $\sum_{j=1}^{l} Q_j \sin^3(j\phi_0) \neq 0$ *holds.*

Set $\rho = \frac{2f'''(0)}{f'(0)} \sum_{j=1}^{l} Q_j \sin(j\phi_0)\big(\cos(j\phi_0) - 1\big)$, *choose* $r \in \{1, \dots, q\}$, *and consider a smooth solution* $\mathcal{B} : \mathbb{R} \times [0, T_*] \to \mathbb{C}$ *of the nonlinear Schrödinger equation with quasi-periodic boundary conditions:*

$$\imath \partial_T \mathcal{B} = \frac{1}{2} \widetilde{\omega}''(\phi_0) \partial_\xi^2 \mathcal{B} + \rho |\mathcal{B}|^2 \mathcal{B}, \qquad \mathcal{B}(\xi+1, T) = \mathrm{e}^{\imath\, 2\pi r/q} \mathcal{B}(\xi, T). \tag{38}$$

Then there exist constants $N_0 \in \mathbb{N}$ *and* $C > 0$ *such that for all* $N \geq N_0$ *with* $\mathrm{e}^{\imath \phi_0 N} = \mathrm{e}^{\imath\, 2\pi r/q}$ *the following holds. If the initial condition* $(\psi_k(0))_{k=1,\dots,N}$ *for system* (36) *satisfies*

$$\|\psi(0) - \varepsilon \Psi_{\mathcal{B}}^{\varepsilon}(0)\|_2 \leq \varepsilon^{3/2}, \qquad \textit{where } \varepsilon = 1/N,$$

then the solution $\psi(t) = (\psi_k(t))_{k=1,\dots,N}$ *of* (36) *satisfies, for all* $t \in [0, T_*/\varepsilon^2]$, *the estimate*

$$\|\psi(t) - \varepsilon \Psi_{\mathcal{B}}^{\varepsilon}(t)\|_2 \leq C \varepsilon^{3/2},$$

where

$$\Psi_{\mathcal{B}}^{\varepsilon}(t) := \Big(\mathcal{B}\big(\varepsilon(k + \widetilde{\omega}'(\phi_0) t), \varepsilon^2 t\big) \mathrm{e}^{\imath(\omega_0 t + \phi_0 k)} + \mathrm{c.c.}\Big)_{k=1,\dots,N}$$

and $\|\psi\|_2 := \big(\sum_1^N \psi_k^2\big)^{1/2}$ *is of order* $\varepsilon^{1/2}$.

Thus, the above result states that the slowly varying amplitude $\mathcal{B}$ of the basic spatially periodic pattern is transported by the group velocity $\omega'(\phi_0)$ and deformed by the Hamiltonian evolution of a family of the nonlinear Schrödinger equations depending on a periodicity parameter; cf. [45]. This reconfirms that the dynamics near the synchronous states is Hamiltonian-like.

8. Discussion.

In this concluding section we point out some general consequences of our results.

(i) *Unidirectional rings are special case of anisotropic coupling:* The case when the ring is unidirectional is important for applications and considered in many works; see, e.g., [17, 43, 79, 50, 13, 66, 54]. The general network (2) is unidirectional when $K_i \neq 0$ for $j = 1, \dots, [(N-1)/2]$ and $K_j = 0$ in other cases. For the forward-backward system (6) the condition for unidirectionality is just $b = 0$. The bifurcation diagram Figure 2 shows that the system dynamics does not change qualitatively with a small variation of coupling parameters. Actually, one can see that the straight line $b = 0$ and lines $b = \pm\epsilon$ intersect bifurcation lines (AH, HC, TC) transversally at almost the same points when ϵ is close to zero. This tells us about the structural stability of the system along parametric line $b = 0$ independently on parameter α.

(ii) *Effects of higher harmonics in the coupling function:* In section 5 we considered examples where the coupling function had only the first term of the Fourier series (27). If the coupling function has higher harmonics, the basic properties related to the symmetries or reversibility of the system remain the same. However, a more complex shape of $g(x)$ can lead to the appearance of new solutions or new bifurcation properties. For instance, for the Hansel–Mato–Meunier [31] coupling function (33) the system (5) has additional fixed points when $|p| \geq 1/2$. If these additional points belong to $\mathrm{Fix}\,\mathcal{R}$, there might appear the same Hamiltonian-like regions around them, similarly as described above.

An example in Figure 3(m) shows that the system of three coupled oscillators with function (33) has four different Hamiltonian-like regions: three of them are bounded by homolinic loops (colored regions in Figure 3(m)) and one is bounded by a Z_3-heteroclinic cycle. These regions coexist with the simply connected dissipative region that includes the sink $\mathcal{M}_1$, the source $\mathcal{M}_2$, and heteroclinic trajectories that connect these two points. Figures 3(n), (o), and (p) illustrate other possible examples. In particular, Figure 3(o) shows how two Hamiltonian-like regions coexist, one of which is homotopic and the other is nonhomotopic to zero.

Appendix.

Proof of Proposition 3.2.

Proof. Let us first rewrite (2) and (5) in the vector form:

$$\dot{\Theta} = F(\Theta), \quad \Theta = (\theta, \dots, \theta_N), \tag{39}$$

and

$$\dot{\Phi} = G(\Phi), \quad \Phi = (\varphi_1, \dots, \varphi_{N-1}). \tag{40}$$

We append the first equation $\dot{\theta}_1 = F_1(\theta_1, \dots, \theta_N) = F_1(\theta_1, \theta_1 - \varphi_1, \dots, \theta_1 - \varphi_{N-1})$ of (39) to (40) and obtain the extended N-dimensional system:

$$\dot{\bar{\Phi}} = \bar{G}(\bar{\Phi}), \quad \bar{\Phi} = (\theta_1, \varphi_1, \dots, \varphi_{N-1}), \tag{41}$$

where

$$\bar{\Phi}^T = \begin{pmatrix} \theta_1 \\ \Phi^T \end{pmatrix} = S_N \Theta^T, \quad S_N = \begin{pmatrix} 1 & 0 & \dots & 0 & 0 \\ 1 & -1 & \ddots & \ddots & 0 \\ \vdots & 0 & \ddots & \ddots & \vdots \\ 1 & \vdots & \ddots & -1 & 0 \\ 1 & 0 & \dots & 0 & -1 \end{pmatrix}. \tag{42}$$

One can check that $\det(S_N) = (-1)^{N-1}$ and $S_N^{-1} = S_N$. The Jacobian matrices at the corresponding points Θ_0, Φ_0, and $\bar{\Phi}_0^T = S_N \Theta_0^T$ are $A = \frac{\partial F}{\partial \Theta}(\Theta_0)$, $B = \frac{\partial G}{\partial \Phi}(\Phi_0)$, and $\bar{B} = \frac{\partial \bar{G}}{\partial \bar{\Phi}}(\bar{\Phi}_0)$. The elements of the Jacobian matrix $A = A(\Theta) = (A_{ij})_{i,j=1,\dots,N}$ are

$$A_{ii} = \sum_{j=1}^{N} K_{j-i} g'(\theta_i - \theta_j) = \sum_{j=1}^{N} K_{j-i} g'(\varphi_{j-1} - \varphi_{i-1}), \quad i = 1, \dots, N,$$
$$A_{ij} = -K_{j-i} g'(\theta_i - \theta_j) = -K_{j-i} g'(\varphi_{j-1} - \varphi_{i-1}), \quad i, j = 1, \dots, N, \ j \neq i.$$

Using the relationship (42) we have $\bar{B} = S_N A S_N^{-1}$. It also holds that

$$\bar{B} = \begin{pmatrix} \bar{B}_{11} & \bar{b} \\ \bar{\bar{b}}^T & B \end{pmatrix},$$

where $\bar{\bar{b}} = 0$, because the right-hand sides $\bar{G}_2, \dots \bar{G}_N$ do not depend on θ_1. Further, the right side of the first equation in (41) is $\bar{G}_1(\bar{\varphi}) = \sum_{j=1}^N K_j g(\varphi_j)$, and it is independent of the variable θ_1, which implies $\bar{B}_{11} = \partial \bar{G}_1/\partial\theta_1 = 0$. Using the above properties we obtain the necessary result:

$$\begin{aligned} \det(A - \lambda I_N) &= \det(S_N^{-1}(\bar{B} - \lambda I_N)S_N) = \det(\bar{B} - \lambda I_N) \\ &= \det \begin{pmatrix} -\lambda & \bar{b} \\ 0 & B - \lambda I_{N-1} \end{pmatrix} = -\lambda \det(B - \lambda I_{N-1}). \end{aligned} \tag{43}$$

■

Proof of Proposition 3.3.

Proof. Let A be the corresponding Jacobian matrix. Direct calculation gives

$$A_{ii}(\mathcal{M}_k) = \sum_{j=1}^N K_{j-i} g'(\mathcal{M}_{k,j-1} - \mathcal{M}_{k,i-1}) = \sum_{j=1}^N K_{j-i}\eta_{k(j-i)} = \sum_{j=1}^N K_j \eta_{kj},$$

$$A_{ij}(\mathcal{M}_k) = -K_{j-i} g'(\mathcal{M}_{k,j-1} - \mathcal{M}_{k,i-1}) = -K_{j-i}\eta_{k(j-i)}, \quad i, j = 1, \dots, N,\ j \neq i,$$

where $\mathcal{M}_{i,j} = \frac{2\pi i}{N} j$ denotes the component of $\mathcal{M}_i$. Since $A(\mathcal{M}_k)$ is circulant, it can be presented as a polynomial of the cyclic permutation matrix

$$P_N = \begin{pmatrix} 0 & 1 & 0 & \dots & 0 \\ 0 & 0 & \ddots & \ddots & \vdots \\ \vdots & \vdots & \ddots & \ddots & 0 \\ 0 & 0 & \dots & 0 & 1 \\ 1 & 0 & \dots & 0 & 0 \end{pmatrix}$$

in the following form:

$$A(\mathcal{M}_k) = \sum_{j=1}^N K_{j-i}\eta_{k(j-i)} I_N - \sum_{j=1}^N K_{j-i}\eta_{k(j-i)} P_N^{j-i} = \sum_{j=1}^N K_j \eta_{kj} \left(I_N - P_N^j\right),$$

where $\eta_{kj} = g'\left(\frac{2\pi k}{N} j\right)$, $k = 0, \dots, N-1$. Eigenvalues of this circulant matrix can be written as

$$\lambda_m(\mathcal{M}_k) = \sum_{j=1}^N K_j \eta_{kj}(1 - \nu_m^j), \quad m = 1, \dots, N,$$

where $\nu_m = \exp\left(\frac{2\pi\imath}{N} m\right)$ are eigenvalues of P_N. Note that equalities $\nu_N^j = \exp\left(\frac{2\pi\imath}{N} jN\right) = 1$ imply $\lambda_N(\mathcal{M}_k) = 0$. ■

Acknowledgments. We thank L. Recke, M. Zaks, A. Pikovsky, M. Rosenblum, and P. Ashwin for useful discussions.

REFERENCES

[1] D. Abrams and S. Strogatz, *Chimera states for coupled oscillators*, Phys. Rev. Lett., 93 (2004), 174102, https://doi.org/10.1063/1.2165594.

[2] V. Afraimovich, P. Ashwin, and V. Kirk, *Robust heteroclinic and switching dynamics*, Dyn. Syst., 25 (2010), pp. 285–286, https://doi.org/10.1080/14689367.2010.522390.

[3] G. E. Alexander, M. R. Delong, and P. L. Strick, *Parallel organization of functionally segregated circuits linking basal ganglia and cortex*, Annu. Rev. Neurosci., 9 (1986), pp. 357–381, https://doi.org/10.1146/annurev.ne.09.030186.002041.

[4] V. Arnold, *Reversible systems*, Nonlinear Turbulent Processes Phys., 3 (1984), pp. 1161–1174.

[5] V. Arnol'd and M. Sevryuk, *Oscillations and bifurcations in reversible systems*, in Nonlinear Phenomena in Plasma Physics and Hydrodynamics, R. Z. Sagdeev, ed., Mir, Moscow, 1986, pp. 31–64.

[6] P. Ashwin, C. Bick, and O. Burylko, *Identical phase oscillator networks: Bifurcations, symmetry and reversibility for generalized coupling*, Front. Appl. Math. Stat., 2 (2016), https://doi.org/10.3389/fams.2016.00007.

[7] P. Ashwin and O. Burylko, *Weak chimeras in minimal networks of coupled phase oscillators*, Chaos, 25 (2015), 013106, https://doi.org/10.1063/1.4905197.

[8] A. Back, J. Guckenheimer, M. Myers, F. Wicklin, and P. Worfolk, *DsTool: Computer assisted exploration of dynamical systems*, Notices Amer. Math. Soc., 39 (1992), pp. 303–309.

[9] W. Baoshe, *Perturbations of lower dimensional tori in the resonant zone for reversible systems*, J. Math. Anal. Appl., 253 (2001), pp. 558–577, https://doi.org/10.1006/jmaa.2000.7165.

[10] I. Belykh and A. Shilnikov, *When weak inhibition synchronizes strongly desynchronizing networks of bursting neurons*, Phys. Rev. Lett., 101 (2008), 078102.

[11] M. Bonnin, *Waves and patterns in ring lattices with delays*, Phys. D, 238 (2009), pp. 77–87, https://doi.org/10.1016/j.physd.2008.08.015.

[12] H. Bosetti, H. A. Posch, C. Dellago, and W. G. Hoover, *Time-reversal symmetry and covariant Lyapunov vectors for simple particle models in and out of thermal equilibrium*, Phys. Rev. E, 82 (2010), 046218, https://doi.org/10.1103/PhysRevE.82.046218.

[13] B. J. Breen, A. B. Doud, J. R. Grimm, A. H. Tanasse, S. J. Tanasse, J. F. Lindner, and K. J. Maxted, *Electronic and mechanical realizations of one-way coupling in one and two dimensions*, Phys. Rev. E, 83 (2011), 037601, https://doi.org/10.1103/PhysRevE.83.037601.

[14] H. Broer, G. Hnitema, and M. Sevryuk, *Families of quasi-periodic motions in dynamical systems depending on parameters*, Progr. Nonlinear Differential Equations Appl., 19 (1996), pp. 171–211.

[15] H. W. Broer, M. C. Ciocci, and H. Hanssmann, *The quasi-periodic reversible hopf bifurcation*, Internat. J. Bifurcation Chaos, 17 (2007), pp. 2605–2623.

[16] H. W. Broer, G. B. Huitema, and M. B. Sevryuk, *Quasi-Periodic Motions in Families of Dynamical Systems*, Springer, New York, 1996.

[17] A. Bulsara, V. In, A. Kho, P. Longhini, A. Palacios, W. Rappel, J. Acebron, S. Baglio, and B. Ando, *Complex behavior in driven unidirectionally coupled overdamped duffing elements*, Phys. Rev. E, 73 (2006), 066121, https://doi.org/10.1103/PhysRevE.73.066121.

[18] J. Collins and I. Stewart, *A group-theoretic approach to rings of coupled biological oscillators.*, Biol Cybern., 71 (1994), pp. 95–103.

[19] H. Daido, *Strange waves in coupled-oscillator arrays: Mapping approach*, Phys. Rev. Lett., 78 (1997), pp. 1683–1686.

[20] G. Van der Sande, M. C. Soriano, I. Fischer, and C. R. Mirasso, *Dynamics, correlation scaling, and synchronization behavior in rings of delay-coupled oscillators*, Phys. Rev. E, 77 (2008), 055202, https://doi.org/10.1103/PhysRevE.77.055202.

[21] R. Devaney, *Reversible diffeomorphisms and flows*, Trans. Amer. Math. Soc., 218 (1976), pp. 89–113.

[22] E. J. Doedel, R. C. Poffenroth, A. R. Champneys, T. F. Fairgrieve, Yu. A. Kuznetsov, B. E. Oldeman, B. Sandstede, and X. Wang, *AUTO-2000: Continuation and Bifurcation Software for Ordinary Differential Equations (with HomCont)*, Technical report, Concordia University, Montreal, QC, 2002.

[23] B. Fiedler and D. Turaev, *Coalescence of reversible homoclinic orbits causes elliptic resonance*, Internat. J. Bifurcation Chaos, 6 (1996), pp. 1007–1027, https://doi.org/10.1142/S0218127496000552.

[24] J.-J. Gervais, *Bifurcations of subharmonic solutions in reversible systems*, J. Differential Equations, 75 (1988), pp. 28–42, https://doi.org/10.1016/0022-0396(88)90127-1.

[25] J. Giannoulis and A. Mielke, *The nonlinear Schrödinger equation as a macroscopic limit for an oscillator chain with cubic nonlinearities*, Nonlinearity, 17 (2004), pp. 551–565.

[26] M. Golubitsky, M. Krupa, and C. Lim, *Time-reversibility and particle sedimentation*, SIAM J. Appl. Math., 51 (1991), pp. 49–72, https://doi.org/10.1137/0151005.

[27] M. Golubitsky and W. F. Langford, *Classification and unfoldings of degenerate Hopf bifurcations*, J. Differential Equations, 41 (1981), pp. 375–415, https://doi.org/10.1016/0022-0396(81)90045-0.

[28] M. Golubitsky and I. Stewart, *Nonlinear dynamics of networks: The groupoid formalism*, Bull. Amer. Math. Soci., 43 (2006), pp. 305–364.

[29] M. Golubitsky and I. Stewart, *Rigid patterns of synchrony for equilibria and periodic cycles in network dynamics*, Chaos, 26 (2016), 094803, https://doi.org/10.1063/1.4953664.

[30] J. Guckenheimer and P. Holmes, *Nonlinear Oscillations, Dynamical Systems, and Bifurcations of Vector Fields*, Springer, New York, 2002.

[31] D. Hansel, G. Mato, and C. Meunier, *Clustering and slow switching in globally coupled phase oscillators*, Phys. Rev. E, 48 (1993), pp. 3470–3477.

[32] F. C. Hoppensteadt and E. M. Izhikevich, *Weakly Connected Neural Networks*, Appl. Math. Sci., Springer, New York, 1997.

[33] M. Kantner and S. Yanchuk, *Bifurcation analysis of delay-induced patterns in a ring of Hodgkin-Huxley neurons*, Phil. Trans. Roy. Soc. A, 371 (2013), 20120470.

[34] T. Kapitaniak, P. Kuzma, J. Wojewoda, K. Czolczynski, and Y. Maistrenko, *Imperfect chimera states for coupled pendula*, Sci. Reports, 4 (2014), 6379, http://dx.doi.org/10.1038/srep06379.

[35] P. Kirrmann, G. Schneider, and A. Mielke, *The validity of modulation equations for extended systems with cubic nonlinearities*, Proc. Roy. Soc. Edinburgh Sect. A, 122 (1992), pp. 85–91.

[36] V. Klinshov, D. Shchapin, S. Yanchuk, and V. Nekorkin, *Jittering waves in rings of pulse oscillators*, Phys. Rev. E, 94 (2016), 012206, https://doi.org/10.1103/PhysRevE.94.012206.

[37] Y. Kuramoto, *Chemical Oscillations, Waves, and Turbulence*, Springer, New York, 1984.

[38] Y. Kuramoto and D. Battogtokh, *Coexistence of coherence and incoherence in nonlocally coupled phase oscillators*, Nonlinear Phenom. Complex Syst., 5 (2002), pp. 380–385, http://www.j-npcs.org/abstracts/vol2002/v5no4/v5no4p380.html.

[39] Y. Kuznetsov, *Elements of Applied Bifurcation Theory*, Appl. Math. Sci. 112, Springer, New York, 1995.

[40] J. S. Lamb and J. A. Roberts, *Time-reversal symmetry in dynamical systems: A survey*, Phys. D, 112 (1998), pp. 1–39.

[41] J. S. Lamb and C. Wulff, *Reversible relative periodic orbits*, J. Differential Equations, 178 (2002), pp. 60–100, https://doi.org/10.1006/jdeq.2001.4004.

[42] J. S. W. Lamb, *Reversing symmetries in dynamical systems*, J. Phys. A, 25 (1992), p. 925, http://stacks.iop.org/0305-4470/25/i=4/a=028.

[43] J. F. Lindner, K. M. Patton, P. M. Odenthal, J. C. Gallagher, and B. J. Breen, *Experimental observation of soliton propagation and annihilation in a hydromechanical array of one-way coupled oscillators*, Phys. Rev. E, 78 (2008), 066604, https://doi.org/10.1103/PhysRevE.78.066604.

[44] I. P. Marino, V. Pérez-Mu nuzuri, V. Pérez-Villar, E. Sánchez, and M. A. Matías, *Interaction of chaotic rotating waves in coupled rings of chaotic cells*, Phys. D, 128 (1999), pp. 224–235.

[45] A. Mielke, G. Schneider, and A. Ziegra, *Comparison of inertial manifolds and application to modulated systems*, Math. Nachr., 214 (2000), pp. 53–69.

[46] J. Moser, *Stable and Random Motions in Dynamical Systems*, Princeton University Press, Princeton, NJ, 1973.

[47] E. Nijholt, B. Rink, and J. Sanders, *Center manifolds of coupled cell networks*, SIAM J. Math. Anal., 49 (2017), pp. 4117–4148, https://doi.org/10.1137/16M106861X.

[48] I. O. Parasyuk, *Conservation of quasiperiodic motions of reversible multifrequency systems*, Dokl. Akad. Nauk Ukrain. SSR, A 9 (1982), pp. 19–22 (in Russian).

[49] P. Perlikowski, S. Yanchuk, O. V. Popovych, and P. A. Tass, *Periodic patterns in a ring of delay-coupled oscillators*, Phys. Rev. E, 82 (2010), 036208, https://doi.org/10.1103/PhysRevE.82.036208.

[50] P. Perlikowski, S. Yanchuk, M. Wolfrum, A. Stefanski, P. Mosiolek, and T. Kapitaniak, *Routes to complex dynamics in a ring of unidirectionally coupled systems*, Chaos, 20 (2010), 013111.

[51] A. Pikovsky and P. Rosenau, *Phase compactons*, Phys. D, 218 (2006), pp. 56–69, https://doi.org/10.1016/j.physd.2006.04.015.
[52] A. Politi, G. L. Oppo, and R. Badii, *Coexistence of conservative and dissipative behavior in reversible dynamical systems*, Phys. Rev. A, 33 (1986), pp. 4055–4060, https://doi.org/10.1103/PhysRevA.33.4055.
[53] O. V. Popovych, S. Yanchuk, and P. A. Tass, *Delay- and coupling-induced firing patterns in oscillatory neural loops*, Phys. Rev. Lett., 107 (2011), 228102, https://doi.org/10.1103/PhysRevLett.107.228102.
[54] S. Rajamani and S. Rajasekar, *Signal amplification by unidirectional coupling of oscillators*, Phys. Scripta, 88 (2013), 015010, http://stacks.iop.org/1402-4896/88/i=1/a=015010.
[55] L. Ren and B. Ermentrout, *Phase locking in chains of multiple-coupled oscillators*, Phys. D, 143 (2000), pp. 56–73, https://doi.org/10.1016/S0167-2789(00)00096-8.
[56] J. A. G. Roberts and G. R. W. Quispel, *Chaos and time-reversal symmetry: Order and chaos in reversible dynamical systems*, Phys. Rep., 216 (1992), pp. 63–177.
[57] H. Sakaguchi and Y. Kuramoto, *A soluble active rotator model showing phase transitions via mutual entrainment*, Prog. Theor. Phys., 76 (1986), pp. 576–581.
[58] E. Sánchez and M. A. Matías, *Experimental observation of a periodic rotating wave in rings of unidirectionally coupled analog lorenz oscillators*, Phys. Rev. E, 57 (1998), pp. 6184–6186, https://doi.org/10.1103/PhysRevE.57.6184.
[59] M. Sevryuk, *Reversible Systems*, Springer Lecture Notes in Math. 1211, Springer, New York, 1986.
[60] M. Sevryuk, *On invariant tori of reversible systems in the neighbourhood of an equilibrium position*, Russian Math. Surv., 42 (1987), pp. 147–148.
[61] M. B. Sevryuk, *The reversible context* 2 *in KAM theory: The first steps*, Regular Chaotic Dynam., 16 (2011), pp. 24–38.
[62] A. Shilnikov, R. Gordon, and I. Belykh, *Polyrhythmic synchronization in bursting networking motifs*, Chaos, 18 (2008), 037120, https://doi.org/10.1063/1.2959850.
[63] L. P. Shilnikov, A. Shilnikov, D. Turaev, and L. Chua, *Methods of Qualitative Theory in Nonlinear Dynamics. Part* II, World Scientific, River Edge, NJ, 2001.
[64] M. C. Soriano, J. Garcia-Ojalvo, C. R. Mirasso, and I. Fischer, *Complex photonics: Dynamics and applications of delay-coupled semiconductors lasers*, Rev. Mod. Phys., 85 (2013), pp. 421–470, https://doi.org/10.1103/RevModPhys.85.421.
[65] J. C. Sprott, W. G. Hoover, and C. G. Hoover, *Heat conduction, and the lack thereof, in time-reversible dynamical systems: Generalized Nosé-Hoover oscillators with a temperature gradient*, Phys. Rev. E, 89 (2014), 042914, https://doi.org/10.1103/PhysRevE.89.042914.
[66] N. Strelkowa and M. Barahona, *Transient dynamics around unstable periodic orbits in the generalized repressilator model*, Chaos, 21 (2011), 023104, https://doi.org/10.1063/1.3574387.
[67] A. Takamatsu, R. Tanaka, H. Yamada, T. Nakagaki, T. Fujii, and I. Endo, *Spatiotemporal symmetry in rings of coupled biological oscillators of physarum plasmodial slime mold*, Phys. Rev. Lett, 87 (2001), 078102, https://doi.org/10.1103/PhysRevLett.87.078102.
[68] D. Topaj and A. Pikovsky, *Reversibility vs. synchronization in oscillator lattices*, Phys. D, 170 (2002), pp. 118–130, https://doi.org/10.1016/S0167-2789(02)00536-5.
[69] K. Y. Tsang, R. E. Mirollo, S. H. Strogatz, and K. Wiesenfeld, *Dynamics of a globally coupled oscillator array*, Phys. D, 48 (1991), pp. 102–112, https://doi.org/10.1016/0167-2789(91)90054-D.
[70] K. Y. Tsang, R. E. Mirollo, S. H. Strogatz, and K. Wiesenfeld, *Reversibility and noise sensitivity of josephson arrays*, Phys. Rev. Lett., 66 (1991), pp. 1094–1097, https://doi.org/10.1103/PhysRevLett.66.1094.
[71] G. Van der Sande, M. C. Soriano, I. Fischer, and C. R. Mirasso, *Dynamics, correlation scaling, and synchronization behavior in rings of delay-coupled oscillators*, Phys. Rev. E, 77 (2008), 055202.
[72] A. Vanderbauwhede, *Local Bifurcation and Symmetry*, Res. Notes Math., Pitman, London, 1982.
[73] D. Wiley, S. H. Strogatz, and M. Girvan, *The size of the sync basin*, Chaos, (2006), 015103.
[74] A. Winfree, *The Geometry of Biological Time*, Springer, New York, 2001.
[75] J. Wojcik, J. Schwabedal, R. Clewley, and A. L. Shilnikov, *Key bifurcations of bursting polyrhythms in* 3*-cell central pattern generators*, PLoS ONE, 9 (2014), e92918, https://doi.org/10.1371/journal.pone.0092918.

[76] M. Wolfrum, O. E. Omel'chenko, S. Yanchuk, and Y. L. Maistrenko, *Spectral properties of chimera states*, Chaos, 21 (2011), 013112, https://doi.org/10.1063/1.3563579.

[77] S. Yanchuk, P. Perlikowski, O. V. Popovych, and P. A. Tass, *Variability of spatio-temporal patterns in non-homogeneous rings of spiking neurons*, Chaos, 21 (2011), 047511, https://doi.org/10.1063/1.3665200.

[78] S. Yanchuk, P. Perlikowski, M. Wolfrum, A. Stefanski, and T. Kapitaniak, *Amplitude equations for collective spatio-temporal dynamics in arrays of coupled systems*, Chaos, 25 (2015), 033113, https://doi.org/10.1063/1.4915941.

[79] S. Yanchuk and M. Wolfrum, *Destabilization patterns in chains of coupled oscillators*, Phys. Rev. E, 77 (2008), 026212, https://doi.org/10.1103/PhysRevE.77.026212.

[80] Y. Zhang, G. Hu, and H. A. Cerdeira, *How does a periodic rotating wave emerge from high-dimensional chaos in a ring of coupled chaotic oscillators?*, Phys. Rev. E, 64 (2001), 037203, https://doi.org/10.1103/PhysRevE.64.037203.

[81] Z. Zhang, *Reducibility of reversible system with small perturbation.*, Ann. Differential Equations, 21 (2005), pp. 629–638.